AGU PUBLICATIONS

Tectonics

RESEARCH ARTICLE
10.1002/2013TC003488

Key Points:
- The Baijiantan and Darbut ophiolites formed in a remnant back-arc ocean basin
- Ophiolites were emplaced in strike-slip faults and were not plate boundaries
- Geochronology, deformation, and magmatism respond to regional plate collisions

Supporting Information:
- Readme
- Text S1
- Table S1

Correspondence to:
Z. Guo,
zjguo@pku.edu.cn

Citation:
Chen, S., G. Pe-Piper, D. J. W. Piper, and Z. Guo (2014), Ophiolitic mélanges in crustal-scale fault zones: Implications for the Late Palaeozoic tectonic evolution in West Junggar, China, *Tectonics*, *33*, 2419–2443, doi:10.1002/2013TC003488.

Received 21 NOV 2013
Accepted 12 NOV 2014
Accepted article online 14 NOV 2014
Published online 11 DEC 2014

Ophiolitic mélanges in crustal-scale fault zones: Implications for the Late Palaeozoic tectonic evolution in West Junggar, China

Shi Chen[1,2], Georgia Pe-Piper[3], David J. W. Piper[4], and Zhaojie Guo[1]

[1]Key Laboratory of Orogenic Belts and Crustal Evolution, Ministry of Education, School of Earth and Space Sciences, Peking University, Beijing, China, [2]State Key Laboratory of Petroleum Resources and Prospecting, College of Geosciences, China University of Petroleum, Beijing, China, [3]Department of Geology, Saint Mary's University, Halifax, Nova Scotia, Canada, [4]Natural Resources Canada, Geological Survey of Canada (Atlantic), Bedford Institute of Oceanography, Dartmouth, Nova Scotia, Canada

Abstract The Baijiantan and Darbut ophiolites in West Junggar are exposed in steep fault zones (>70°) containing serpentinite mélange, in contact on either side with regionally distributed Upper Devonian-Lower Carboniferous ocean floor peperitic basalts and overlying sedimentary successions. The ophiolitic mélanges show classic structural features created by strike-slip faulting and consistent shear sense indicators of left-slip kinematics. Sandstone blocks within the mélanges resemble the surrounding sediments in lithology and age, indicating that the ophiolitic mélanges consist of locally derived rocks. The ophiolitic mélanges therefore originated from left-slip fault zones within a remnant basin and are not plate boundaries nor subduction suture zones. Sandstone is the youngest lithology involved in the mélange and provides a maximum age for the mélange of 322 Ma, whereas stitching plutons are younger than 302 Ma. Multiple clusters in zircon ages from single gabbro blocks in the mélange at ~375, ~360, ~354, and ~340 Ma are inconsistent with accretionary incorporation of subducting ocean crust but rather suggest that episodic movement of the faults provided pathways for magma from the mantle into magma chambers. Late Paleozoic tectonic evolution of West Junggar involved Late Devonian to Carboniferous relative motion between the Junggar block and West Junggar ocean basin, which triggered the left-slip fault zones within a remnant ocean basin, along which the oceanic crust was disrupted to form linear ophiolitic mélanges. Final filling of this remnant ocean basin and its dismemberment by strike-slip faulting occurred in the late Carboniferous, followed by crustal thickening by juvenile granites at the Carboniferous-Permian boundary.

1. Introduction

Ophiolitic mélanges are defined as tectonic and olistostromal mixing of ophiolitic blocks into serpentinitic or pelagic and flyschoidal matrix materials [*Gansser*, 1974]. Generally, the ophiolitic mélanges are often overthrusted by ultramafic or ophiolitic nappes and mark major suture zones within continental crust, because they represent the remnants of accreted fragments of vanished oceans. Therefore, ophiolites and/or mélanges found in the field are usually regarded as sutures [*Dewey*, 1977, 2005; *Smith and Colchen*, 1988; *Şengör*, 1992; *Xiao et al.*, 2014]. However, some ophiolitic mélanges, as stressed by *Gansser* [1974] and *Orange* [1990] may develop in shear zones or by diapirism from deep-ocean fracture zones. Therefore, the question arises as to whether all ophiolites and/or ophiolitic mélanges found in the field are all sutures.

The Central Asian Orogenic Belt (CAOB), also termed the Altaid tectonic collage or Central Asian Orogenic System [*Şengör et al.*, 1993; *Şengör and Natal'in*, 1996; *Yakubchuk*, 2004; *Briggs et al.*, 2007, 2009], is one of the largest Phanerozoic accretionary orogens in the world. It extends about 5000 km from the Urals in the west to the Sikhote-Alin' in the Russian Far East, where it is truncated by Mesozoic Pacific subduction-accretion systems, and separates the Siberian craton from the Tarim and North China cratons (Figure 1a). The belt was formed by Neoproterozoic-Paleozoic successive amalgamation of allochthonous oceanic and pericratonic terranes, island arcs, and possibly microcontinents [*Coleman*, 1989; *Jahn*, 2004; *Windley et al.*, 2007; *Xiao et al.*, 2008]. The Central Asian Orogenic Belt has been divided into two domains: the western Kazakhstan-Tianshan and the eastern Altai-Mongol domains, which are characterized by the formation of the horseshoe-shaped belts, the Kazakhstan orocline (Figure 1b) and the Tuva-Mongol orocline [*Şengör and Natal'in*, 1996; *Buslov et al.*, 2001; *Collins et al.*, 2003; *Levashova et al.*, 2003; *Abrajevitch et al.*, 2007; *Windley et al.*, 2007; *Xiao et al.*, 2010].

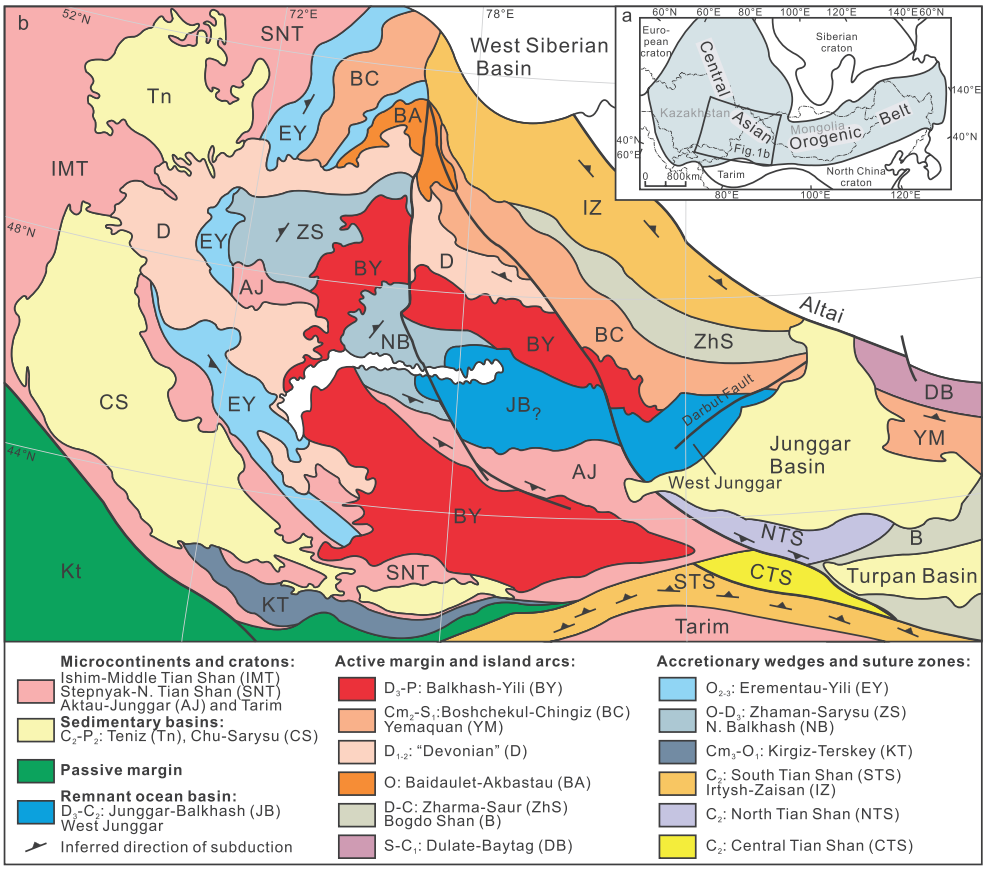

Figure 1. (a) Simplified sketch map of the Central Asian Orogenic Belt (modified after *Şengör et al*. [1993] and *Jahn* [2004]). (b) Geological map of the Kazakhstan part of the Western Altaids in the Paleozoic (modified after *Windley et al*. [2007] and *Xiao et al*. [2010]).

The North Xinjiang region of western China occupies the junction of the Kazakhstan orocline and Tuva-Mongol oroclines [*Xiao et al*., 2010], a key area to better understand the tectonic evolution of the CAOB. A series of ophiolitic belts were identified in North Xinjiang (Figure 2). Most ophiolitic belts in North Xinjiang trend in a northwest to west-northwest direction, but in West Junggar the ophiolitic belts trend northeast, represented by the Darbut (also called Dalabute) and Baijiantan (or Keramay) ophiolitic belts (Figure 2).

The West Junggar region is situated in the easternmost inner end of the Kazakhstan orocline [*Windley et al*., 2007; *Xiao et al*., 2010] (Figure 1b) and has been considered to be part of the triple junction where the Siberian, Tarim, and Kazakhstan plates are sutured [e.g., *Feng et al*., 1989]. Many tectonic models have also been proposed based on the assumption that these two ophiolitic belts represented suture zones as parts of an accretionary complex. However, new evidence reported by *Chen et al*. [2013] contradicted previously postulated subduction-accretionary mechanisms for the formation of the Darbut and Baijiantan ophiolitic belts. Both ophiolitic belts are bounded by thick, regionally distributed Upper Devonian-Lower Carboniferous ocean floor peperitic basalts and overlying deepwater sedimentary successions (Figures 2 and 3) [*Chen et al*., 2013], which signify a continuous small ocean basin in the Late Devonian to Early Carboniferous of West Junggar. Therefore, a clearer understanding of these two ophiolitic belts is crucial for the tectonic reconstruction of West Junggar and the CAOB.

In this paper, based on a detailed field study, we describe the field relationships and structural patterns of the Darbut and Baijiantan ophiolitic belts in order to document that neither belt is the product of subduction or obduction of oceanic crust at a plate boundary. We demonstrate that the two ophiolitic mélanges represent oceanic crust disrupted along younger left-slip fault zones in a continuous ocean basin in West Junggar. On the basis of new geochronology and multiscale structural analysis, we propose a model for the Late Paleozoic tectonic evolution of West Junggar as a remnant oceanic basin subsequently deformed by strike-slip faulting.

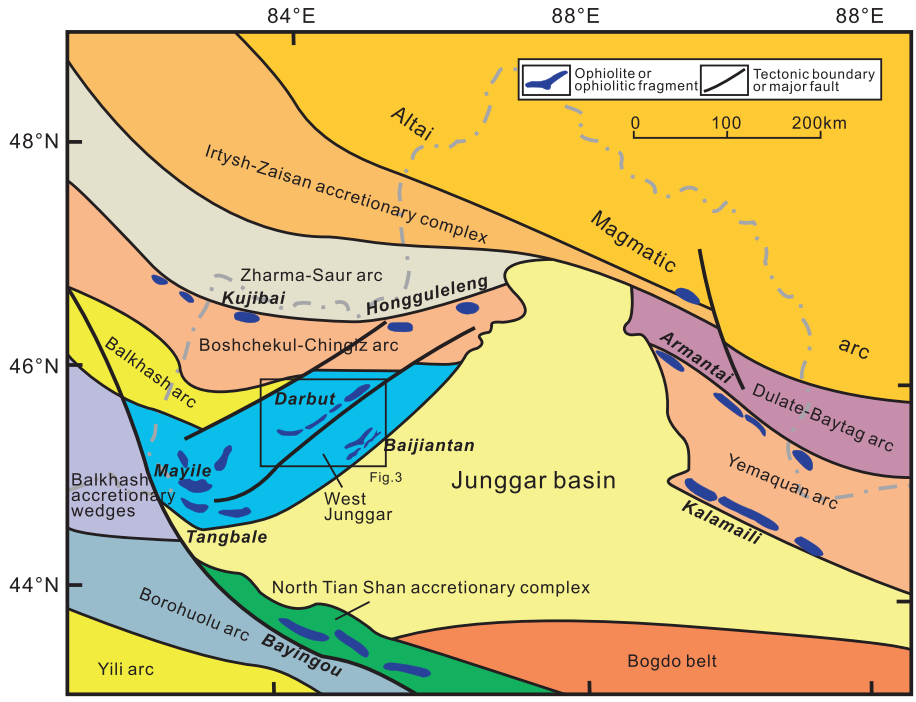

Figure 2. Tectonic map showing the terranes separated by major suture zones and ophiolitic fragments in North Xinjiang and eastern Kazakhstan (modified after *Xiao et al.* [2010] and *Windley et al.* [2007]).

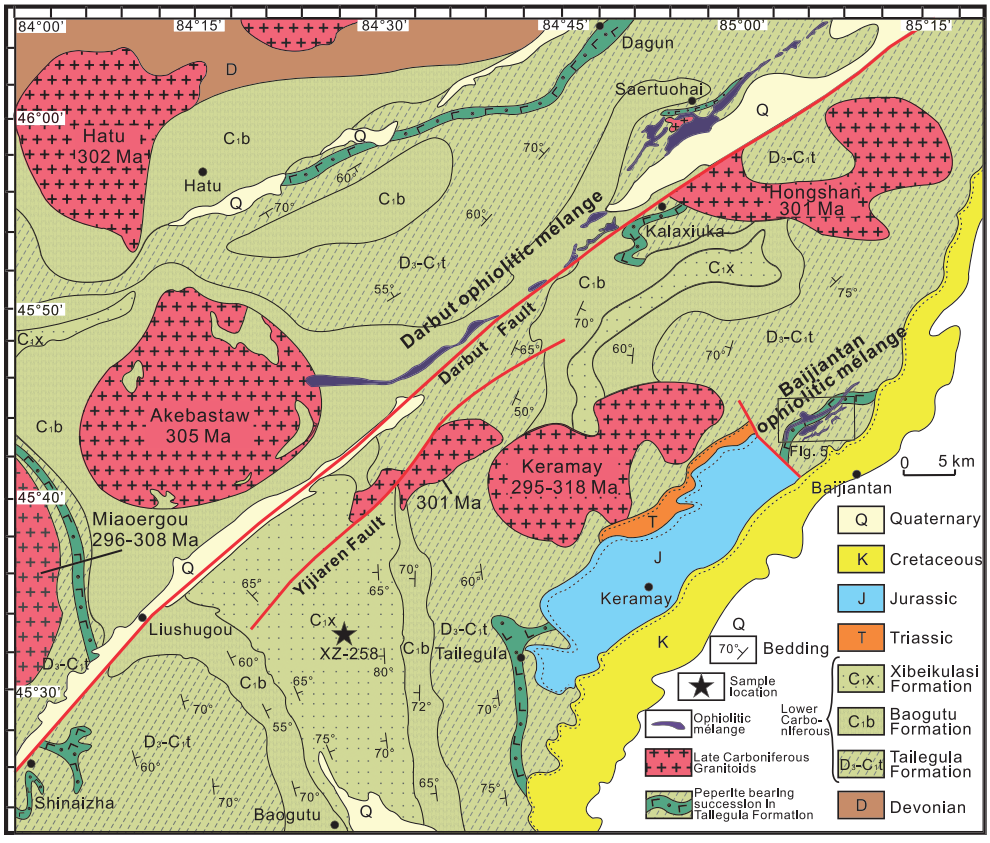

Figure 3. Geologic map of West Junggar (modified after the 1:200,000 geologic map produced by *BGMRXUAR* [1966]). Geochronology data of Upper Carboniferous granitoid plutons from *Han et al.* [2006] and *Geng et al.* [2009].

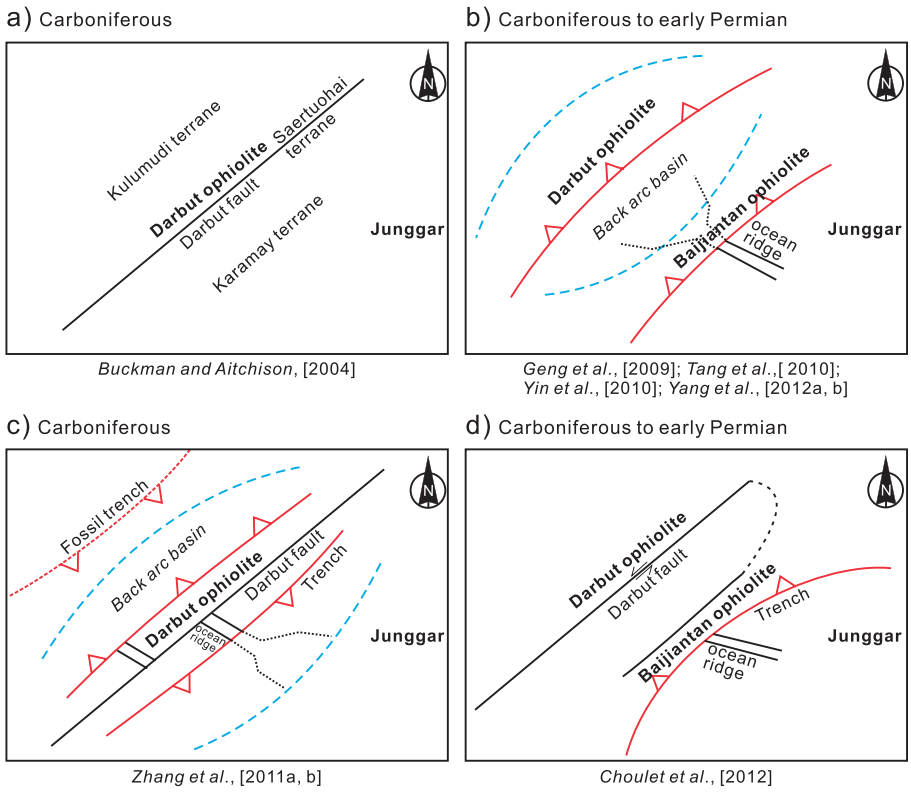

Figure 4. Sketch diagrams illustrating Late Paleozoic tectonic models of the West Junggar proposed by previous studies. (a) Model with one accretionary complex consisting of three separate terranes [*Buckman and Aitchison*, 2004]. (b) NW directed ridge subduction model proposed by *Geng et al.* [2009], *Tang et al.* [2010], and *Yin et al.* [2010] with a second northwestward subduction of Darbut back-arc ocean proposed by *Yang et al.* [2012a, 2012b]. (c) Double subduction along the Darbut ophiolitic belt proposed by *Zhang et al.* [2011a, 2011b]. (d) One transcurrent strike-slip fault displaced one single ophiolitic belt as a result of oblique ridge subduction into two present parallel ophiolitic belts [*Choulet et al.*, 2012a]. See text for detailed interpretation.

2. Geological Setting

In the central and northwestern parts of Central Asia, horseshoe-shaped volcanic belts are the largest structural units in the Kazakhstan orocline (Figure 1b), which was configured by the characteristic oroclinal bending resulting from the convergence of the large cratonic blocks of Baltica, Siberia, and Tarim [*Xiao et al.*, 2010; *Levashova et al.*, 2012]. The Kazakhstan orocline is mainly composed of Devonian to Carboniferous volcanic arcs lying on pre-Devonian microcontinents and volcanic arcs. The North Xinjiang region corresponds to the easternmost extension of the Kazakhstan orocline, which was formed by a progressive southward amalgamation, as indicated by a series of ophiolitic belts outcropping around the Junggar basin, which is covered by Mesozoic and Cenozoic sediments (Figure 2) [*Şengör and Natal'in*, 1996; *Windley et al.*, 2007]. The tectonic attributes of the basement of the Junggar Basin are under debate. It has been interpreted a collage of early Paleozoic arcs, accretionary complexes, trapped oceanic crust, and continental fragments [*Li et al.*, 2000; *Chen and Jahn*, 2004; *Zheng et al.*, 2007; *Li et al.*, 2007; *Xiao et al.*, 2008]. In this study, we consider that it acted as a microcontinent by the Late Devonian. We assume that the microcontinent is a composite consolidated tectonic block (Junggar block) and is probably not a Precambrian craton.

From north to south, the ophiolitic belts in North Xinjiang are: the Kujibai-Hongguleleng ophiolitic belt on the north side of Junggar Basin, the Armantai, and Kalamaili ophiolitic belts on the east side of the Junggar Basin, the Darbut, and Baijiantan ophiolitic belts in West Junggar and the Bayingou ophiolitic belt along the northern edge of the Chinese Tian Shan (Figure 2). The Armantai ophiolite correlates with the Kujibai-Hongguleleng ophiolite as a single E-W Early Ordovician ophiolitic belt extending from east to west in North Xinjiang, and separating the Early Carboniferous Zharma-Saur arc and the Silurian to Early Carboniferous Dulate-Baytag arc in the north from the Silurian Boshchekul-Chingiz arc and the Devonian to

Table 1. SHRIMP U-Pb Data of Zircons From Gabbro Block (Sample XZ10-23) in the Baijiantan Ophiolitic Mélange[a]

Spot	U ppm	Th ppm	$^{206}Pb^{*}$ ppm	$^{206}Pb_c$ %	$^{232}Th/^{238}U$	$^{238}U/^{206}Pb$	Error% (1σ)	$^{207}Pb/^{206}Pb$	Error% (1σ)	$^{206}Pb/^{238}U$ Age (Ma)	
XZ10-23-1.1	10	0	0.468	2.07	0.04	18.15	3.3	0.0665	8.8	340	±11
XZ10-23-2.1	14	3	0.642	1.33	0.20	18.33	3.4	0.0658	6.3	337	±12
XZ10-23-3.1	29	5	1.48	0.65	0.17	17.00	3.0	0.0573	4.4	367	±11
XZ10-23-4.1	15	1	0.806	3.66	0.06	16.32	2.8	0.0653	6.6	378	±11
XZ10-23-5.1	4	0	0.214	6.89	0.07	16.52	4.7	0.0902	11	362	±17
XZ10-23-6.1	7	3	0.366	2.00	0.38	16.54	5.2	0.0724	9.5	370	±19
XZ10-23-7.1	22	2	0.998	0.95	0.10	18.8	7.2	0.0569	6.1	332	±23
XZ10-23-8.1	8	1	0.378	3.25	0.07	18.01	3.7	0.0692	9.6	342	±13
XZ10-23-9.1	17	2	0.883	1.78	0.13	16.66	2.6	0.0617	6.0	372.3	±9.6
XZ10-23-10.1	17	2	0.884	2.61	0.13	16.84	2.7	0.0620	6.3	368.2	±9.9
XZ10-23-11.1	14	2	0.708	2.86	0.14	17.58	3.0	0.0683	6.0	350	±11
XZ10-23-12.1	4	0	0.203	4.79	0.05	16.62	5.2	0.076	14	366	±20
XZ10-23.13.1	9	1	0.498	2.30	0.09	16.35	3.2	0.0659	7.8	377	±12
XZ10-23.14.1	110	46	5.41	0.41	0.43	17.43	2.0	0.0552	2.3	359.0	±7.1
XZ10-23.15.1	133	42	6.63	0.27	0.33	17.29	1.7	0.0550	2.2	361.9	±6.0
XZ10-23.16.1	67	15	3.21	0.27	0.24	17.80	1.8	0.0564	2.8	351.2	±6.3
XZ10-23-17.1	9	1	0.457	3.57	0.09	16.55	3.3	0.0728	7.3	370	±12
XZ10-23-18.1	6	3	0.252	6.27	0.53	19.51	4.3	0.0903	8.8	307	±13
XZ10-23-19.1	16	2	0.812	4.31	0.12	16.61	2.6	0.0765	5.3	366.6	±9.7
XZ10-23-20.1	4	0	0.206	11.40	0.07	16.50	4.7	0.100	10	358	±17

[a]Note that $^{206}Pb^{*}$ and $^{206}Pb_c$ indicate the radiogenic and common Pb content. The $^{238}U/^{206}Pb$ and $^{207}Pb/^{206}Pb$ ratios of all zircons are given uncorrected for common Pb. The ages of zircons are shown as $^{206}Pb/^{238}U$ ages after common Pb correction by the ^{207}Pb method.

Early Carboniferous Yemaquan arc in the south [*Zhang and Guo*, 2010] (Figure 2). The Boshchekul-Chingiz arc comprises Silurian volcanic and siliciclastic sequences cut by Upper Silurian to Lower Devonian intrusions [*Chen et al*., 2010; *Choulet et al*., 2012b, 2012c]. Silurian granites in the Yemaquan arc [*Li et al*., 2009; *Guo et al*., 2009; *Zhang et al*., 2013] imply correlation with the Boshchekul-Chingiz arc. The Kalamaili ophiolitic belt in East Junggar separates the Yemaquan arc in the north from the Junggar basin in the south and the Bayingou ophiolitic belt separates the Junggar basin in the north from the Yili arc in the south (Figure 2).

The West Junggar region is located along the Kazakhstan border in North Xinjiang and bounded to the south by the North Tianshan orogen. The Balkhash arc to the west is conterminous with the Yili arc as a part of Kazakhstan orocline (Figure 1b) [*Windley et al*., 2007; *Yi et al*., 2013]. The principal rock assemblages in West Junggar include Paleozoic ophiolitic mélanges and Carboniferous sedimentary formations, both of which are intruded by sub-circular Upper Carboniferous granitoid plutons with strongly positive ε_{Nd} [*Chen and Arakawa*, 2005] (Figure 3). Regionally, Upper Devonian (circa 364 Ma) peperitic basalt lavas are interbedded with sedimentary rocks including chert, and pass up into a 5 km thick Carboniferous succession of shallowing-up clastic facies that include some volcanic rocks. These continuous stratigraphic sections have been divided into the Tailegula, Baogutu, and Xibeikulasi formations from the bottom up [*Chen et al*., 2013] and are distributed regionally over a distance of 100 km on both sides of the Darbut fault (Figure 3). The northeast-striking Darbut fault is known as a Permian and younger high-angle transcurrent strike-slip fault across the whole West Junggar region [*Allen et al*., 1995], extending more than 200 km (Figures 2 and 3).

The most striking geological feature in the West Junggar region is the outcrop of two parallel NE trending subvertical belts of ophiolitic rocks, principally serpentinite: the Baijiantan and Darbut ophiolitic mélanges (Figure 3), forming part of the West Karamay unit [*Zhang et al*., 2011a; *Choulet et al*., 2012a]. Both mélanges have high-angle fault contacts with the surrounding Carboniferous continuous stratigraphic sections. A minimum age for these Carboniferous sedimentary rocks is provided by detrital zircon ages of 307 ± 7 Ma [*Choulet et al*., 2012a]. A Sm-Nd isochron age of 395 ± 12 Ma [*Zhang and Huang*, 1992] and a laser ablation inductively coupled plasma mass spectrometry (LA-ICP-MS) zircon U-Pb age of 391 ± 6 Ma [*Gu et al*., 2009] were obtained from gabbroic rocks within the Darbut ophiolite. Two sets of sensitive high-resolution ion microprobe (SHRIMP) zircon U-Pb dates of 332 ± 14 Ma and 414 ± 9 Ma were reported from a gabbro from the Baijiantan ophiolite [*Xu et al*., 2006b]. The Darbut ophiolitic belt is intruded by the Yegezikala monzogranite with a zircon U-Pb age of 308 ± 3 Ma [*Chen and Guo*, 2010] and the Akebastaw alkali-feldspar granite with a zircon U-Pb age of 305 ± 4 Ma [*Geng et al*., 2009]. The Baijiantan ophiolitic belt is cut by a diorite dike with an amphibole ^{39}Ar-^{40}Ar age of 307 ± 3 Ma [*Zhang et al*., 2011a].

The Paleozoic tectonic evolution of West Junggar principally relies on the interpretation of how these two ophiolitic belts formed. Previous workers assumed that the ophiolitic mélanges were major plate boundaries or subduction suture zones, so that the Upper Devonian

Table 2. SHRIMP U-Pb Data of Zircons From Gabbro Block (Sample XZ10-50) From the Darbut Ophiolitic Mélange[a]

Spot	U ppm	Th ppm	$^{206}Pb^{*}$ ppm	$^{206}Pb_c$ %	$^{232}Th/^{238}U$	$^{207}Pb/^{206}Pb^{*}$	Error% (1σ)	$^{207}Pb^{*}/^{235}U$	Error% (1σ)	$^{206}Pb^{*}/^{238}U$	Error% (1σ)	Error Correlation	$^{206}Pb/^{238}U$ Age (Ma)	
xz10-50-1.1	11	1	0.491	5.88	0.09	0.015	83	0.105	83	0.0494	4.1	.049	311	±12
xz10-50-2.1	148	56	7.09	0.31	0.39	0.0497	3.4	0.382	3.7	0.05574	1.4	.382	349.6	±4.8
xz10-50-3.1	92	46	4.44	0.50	0.52	0.0509	4.8	0.394	5.1	0.05612	1.6	.308	352.0	±5.4
xz10-50-4.1	140	63	7.15	0.55	0.47	0.0505	5.1	0.413	5.3	0.05924	1.5	.278	371.0	±5.3
xz10-50-5.1	76	23	3.67	0.00	0.31	0.0515	3.6	0.400	4.0	0.05631	1.7	.423	353.1	±5.8
xz10-50-6.1	169	41	7.77	0.00	0.25	0.0547	2.4	0.403	2.8	0.05340	1.4	.496	335.3	±4.5
xz10-50-7.1	162	63	7.52	0.71	0.40	0.0504	5.8	0.372	6.0	0.05357	1.7	.277	336.4	±5.5
xz10-50-8.1	190	49	8.85	0.19	0.27	0.0522	2.5	0.389	2.9	0.05411	1.4	.482	339.7	±4.6
xz10-50-9.1	374	46	17.4	--	0.13	0.0554	1.8	0.4151	2.2	0.05434	1.2	.556	341.1	±4.1
xz10-50-10.1	331	148	15.2	0.47	0.46	0.0526	4.7	0.385	4.9	0.05311	1.3	.258	333.6	±4.1
xz10-50-11.1	129	67	5.81	0.42	0.54	0.0515	4.2	0.369	4.4	0.05207	1.5	.332	327.2	±4.7
xz10-50-12.1	228	105	11.9	--	0.48	0.05201	1.9	0.4341	2.3	0.06054	1.3	.563	378.9	±4.7
xz10-50-13.1	301	218	3.11	0.53	0.75	0.0457	5.5	0.0754	5.8	0.01197	1.9	.321	76.7	±1.4
xz10-50-14.1	54	6	2.48	0.00	0.12	0.0532	4.2	0.391	4.9	0.0533	2.5	.508	334.7	±8.1
xz10-50-15.1	197	105	9.47	--	0.55	0.0522	2.1	0.4027	2.5	0.05595	1.3	.535	350.9	±4.5
xz10-50-16.1	141	38	6.60	0.17	0.28	0.0494	3.9	0.370	4.1	0.05439	1.4	.342	341.4	±4.7
xz10-50-17.1	120	24	6.25	0.21	0.20	0.0497	2.8	0.414	3.2	0.06044	1.4	.443	378.3	±5.2
xz10-50-18.1	84	33	4.17	0.52	0.41	0.0482	5.4	0.382	5.6	0.05750	1.6	.277	360.4	±5.5
xz10-50-19.1	330	90	15.5	--	0.28	0.05462	1.6	0.4129	2.0	0.05482	1.2	.610	344.1	±4.1
xz10-50-20.1	72	76	3.40	0.39	1.09	0.0531	6.7	0.401	6.9	0.05475	1.7	.248	343.6	±5.7
xz10-50-21.1	167	63	7.79	0.50	0.39	0.0494	4.6	0.367	4.8	0.05390	1.4	.288	338.4	±4.6
xz10-50-22.1	48	27	2.22	0.00	0.59	0.0500	5.4	0.373	5.7	0.0541	1.9	.324	339.6	±6.1
xz10-50-23.1	58	28	2.60	1.12	0.49	0.0433	8.0	0.308	8.2	0.05156	1.9	.231	324.1	±6.0
xz10-50-24.1	144	28	7.44	0.50	0.20	0.0522	4.1	0.431	4.5	0.0600	1.8	.396	375.5	±6.5
xz10-50-25.1	7	8	0.387	4.97	1.15	0.053	20	0.430	20	0.0593	3.9	.192	371	±14
xz10-50-26.1	16	9	0.879	0.93	0.58	0.0532	11	0.452	12	0.0616	2.6	.224	385.4	±9.9
xz10-50-27.1	87	74	4.26	--	0.88	0.0533	5.1	0.421	5.3	0.05732	1.6	.297	359.3	±5.5
xz10-50-28.1	111	43	5.27	0.35	0.40	0.0519	3.6	0.393	3.9	0.05494	1.5	.379	344.8	±5.0

[a]Note that $^{206}Pb^{*}$ and $^{206}Pb_c$ indicate the radiogenic and common Pb content. The ages of zircons are shown as $^{206}Pb/^{238}U$ ages after common Pb correction by the ^{204}Pb method.

to Carboniferous sedimentary rocks and mélanges were parts of an accretionary complex formed during late Paleozoic subduction (Figure 4).

Some researchers proposed that West Karamay unit represents an accretionary complex [*Buckman and Aitchison*, 2004], consisting of three separate terranes: (1) the Kulumudi terrane to the west, (2) the Karamay terrane to the east, and (3) the Saertuohai terrane, equivalent to the Darbut mélange lying in between them (Figure 4a).

Recently, a Late Carboniferous to early Permian NW directed ridge subduction was proposed beneath the eastern part of West Junggar [*Geng et al*., 2009; *Jin and Zhang*, 1993; *Liu et al*., 2009; *Tang et al*., 2010; *Yin et al*., 2010]. Furthermore, *Yang et al*. [2012a, 2012b] concurred with this model and suggested a two northwestward subduction model along Darbut and Baijiantan ophiolitic belts (Figure 4b).

Zhang et al. [2011a, 2011b] suggested that a back-arc basin extended beyond the Darbut to Baijiantan area and the basin finally was destroyed by double subduction along Darbut ophiolitic belt in the Carboniferous (Figure 4c). The southeastern and northwestern domains on either side of the Darbut fault (Figure 3) represent two separate accretionary complexes in this model.

Choulet et al. [2012a] interpreted the ophiolitic mélanges and sedimentary series in West Junggar as a single Carboniferous accretionary complex that was then split by the Permian transcurrent Darbut fault (Figure 4d). The Darbut (Dalabute) and Baijiantan (Karamay) ophiolitic belts were suggested to be a single flat-lying Early Carboniferous accretionary mélange, later offset ~110 km along the Darbut fault [*Choulet et al*., 2012a].

3. Methods

Our fieldwork includes detailed mapping of the Baijiantan and Darbut ophiolitic belts, mesoscopic structure investigations based on field observations and microscopic study of oriented thin sections, and the collection of samples for subsequent laboratory study. Conventional thin sections were prepared for petrographic analysis. Two samples from gabbro blocks (XZ10-23 and XZ10-50) were collected for geochronology using zircon SHRIMP U-Pb dating (Tables 1 and 2). Three samples from sandstone blocks (XZ10-67, XZ-56, and XZ10-32) and one autochthonous sandstone

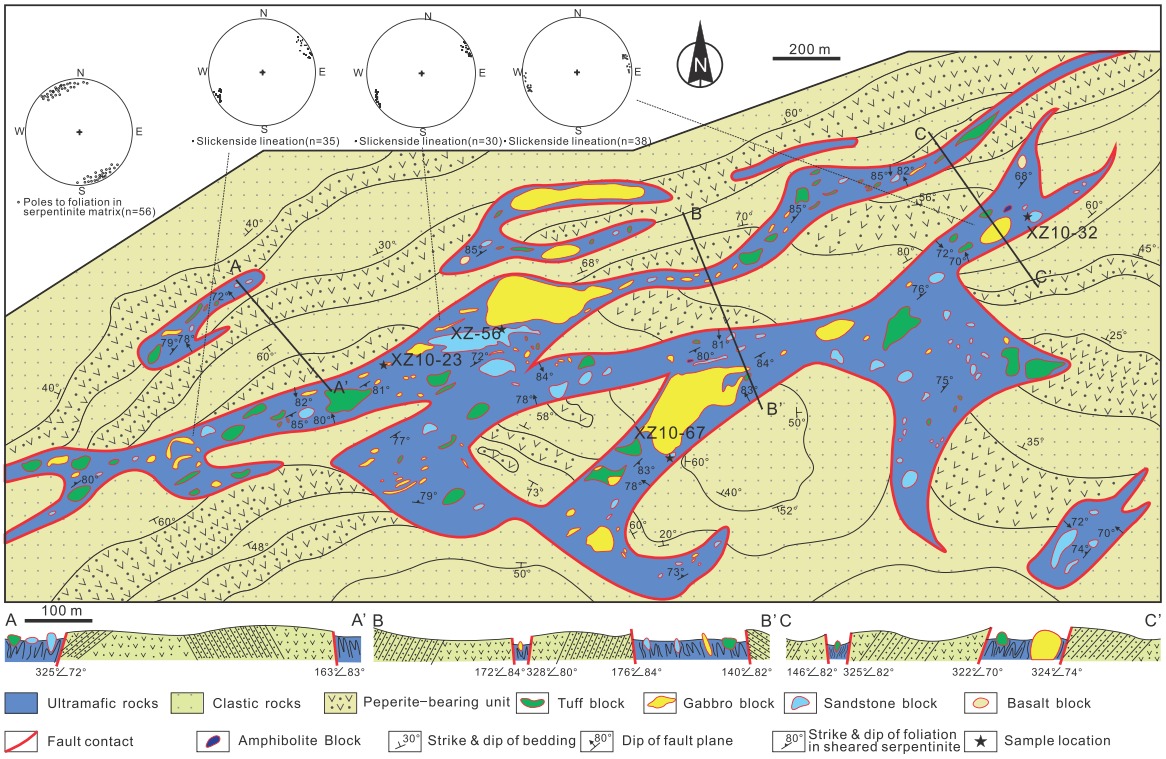

Figure 5. Detailed geological map and cross sections of part of the Baijiantan ophiolitic mélange and its cross sections. Lower hemisphere projections showing the slickenside lineations at different places and poles to foliation in serpentinite matrix within the Baijiantan ophiolitic mélange.

(XZ-258) were also collected for geochronology using zircon LA-ICP-MS U-Pb dating (Table S1 in the supporting information). Detailed description of the preparation procedures and the techniques for zircon SHRIMP U-Pb and LA-ICP-MS dating methods are provided in Text S1 in the supporting information.

4. Field Relationships and Lithologies of the Ophiolitic Mélanges

4.1. Baijiantan Ophiolitic Mélange

The Baijiantan ophiolitic mélange zone ranges in width from 0.5 to ~2 km. Structures of the mélange are dominated by two steeply dipping master fault zones which extend N50°E for about 7 km and a few branch faults (Figure 5). The faults zones are characterized by elongated blocks within a foliated serpentinite matrix that makes up ~50% of the fault zone material (Figure 7a). The proportions of individual lithological block types and the ratio of the matrix to blocks do not change macroscopically along and across the strike of the fault zones. Thousands of tectonic blocks are exposed, which range from 1 cm^2 to ~60,000 m^2 in two dimensions, with most less than 200 m^2. Many are too small to be mapped. The blocks generally are asymmetric lenticular and oblate ellipsoids and dip steeply to NW and SE (Figure 5). No remnant stratigraphy appears to be preserved. Lithologies of the blocks include peridotite, gabbro, volcanic, and sedimentary rocks.

Ultramafic Rocks. Ultramafic rocks include harzburgite, lherzolite, dunite, and a small quantity of pyroxenite. Nearly all the peridotite is serpentinized and foliated to form the matrix of mélange, but some small blocks retain their original mantle lithology. Foliated serpentinite is present along several steeply dipping faults (Figures 5, 7b, and 7c). Some small blocks of peridotite are mylonitic (Figure 7d) and strongly foliated (Figure 7e).

Gabbro. Blocks of gabbro generally underwent prehnitization, epidotization, and chloritization and many are metasomatized to rodingite. A few blocks contain cumulate gabbro sequences.

Pods (~10 m long) of medium to fine grained amphibolites are encased in serpentinite and display relict gabbroic textures and amphibolite-facies assemblages. The Baijiantan ophiolitic mélange includes

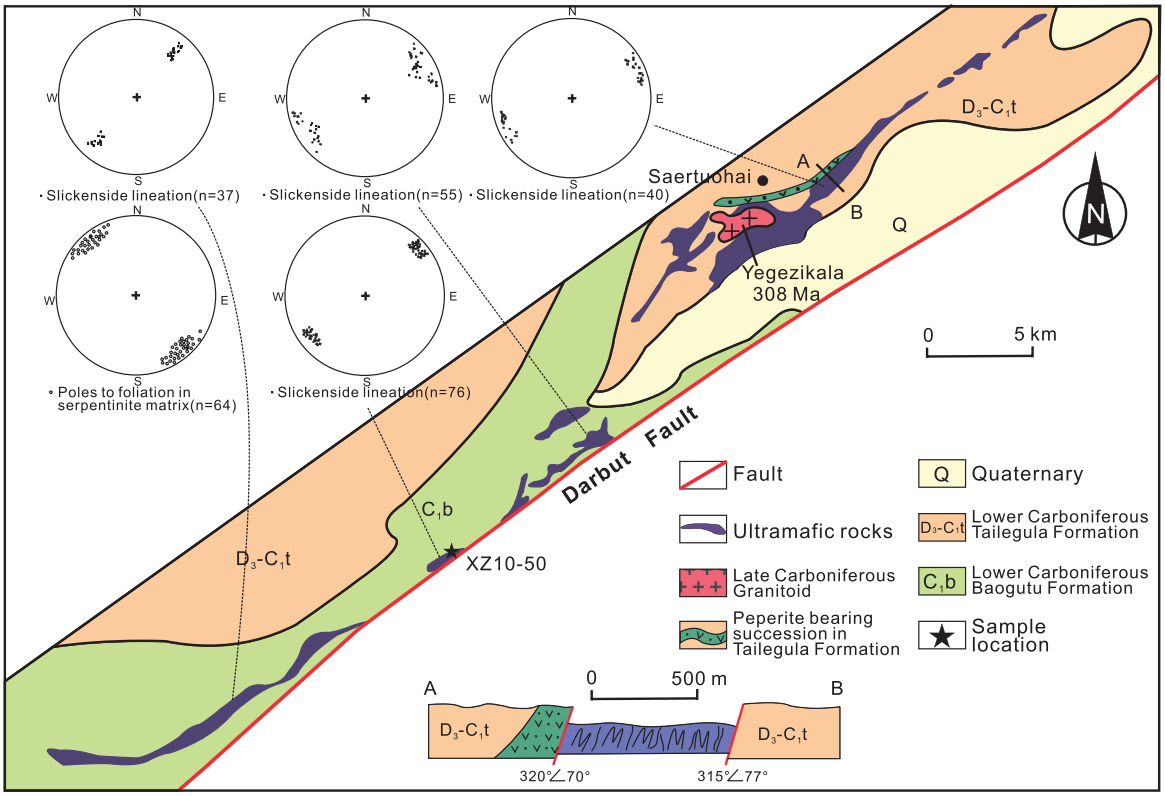

Figure 6. Geological map and cross sections of the Darbut ophiolitic mélange and its cross sections. Lower hemisphere projections showing the slickenside lineations at different places and poles to foliation in serpentinite matrix within the Darbut ophiolitic mélange.

amphibolite breccias consisting of centimeter-sized mylonitic amphibolite clasts embedded within a serpentinite matrix (Figure 7f). Most clasts within the amphibolite breccias are between 0.5 and 5 cm with sharp edges. The clasts exhibit a marked mylonitic foliation which is discordant with the contacts with the matrix and the foliation in the serpentinite matrix, indicating metamorphism of the amphibolite took place prior to brittle deformation that generated the sharp clasts.

Volcanic Rocks. Volcanic rocks cropping out in the Baijiantan ophiolitic mélange are of two types: type 1 and type 2 lavas. The type 1 lavas, generally altered to greenschist assemblages but succeeded by prehnite-pumpellyite facies in some metabasalts, occur within the fault zones as small blocks within the matrix of ultramafic rocks, which have mid-ocean ridge basalt (MORB)-like geochemical features [*Zhang et al*., 2011b; *Yang et al*., 2012a]. Some blocks include associated cherts that contain Devonian radiolarian fossils [*Feng et al*., 1989]. All examples of type 1 lavas are tectonically juxtaposed against other rocks.

The type 2 basalt lava, including peperites and pillow lavas and sedimentary rocks containing chert, regionally forms a continuous stratigraphic section at the bottom of the Carboniferous succession. A relatively undeformed NE trending peperite-bearing succession outcrops between Tailegula and Baijiantan, unconformably overlain by Jurassic strata, and is in tectonic contact with and deformed along with the belts of ophiolitic mélange via high-angle faults in Baijiantan (Figures 3 and 5). Mixed basalt and sedimentary rocks and some typical outcrops of peperite occur as blocks in a matrix of serpentinized ultramafic rocks in Baijanatan (Figures 7g and 7h).

Sedimentary Rocks. Besides the volcanic rocks, the other supracrustal rocks in the ophiolitic mélange include sandstone, chert, tuff, and very rare limestone. Sandstone and minor tuff make up 50% of the ophiolitic belt (Figure 5), and their characteristics are consistent with the sandstones and tuff from surrounding Lower Carboniferous sedimentary formations. Most sandstone is fine grained and tuffaceous, similar to the flysch. of the Tailegula Formation. Sedimentary structures such as cross bedding and lenticular bedding (Figures 7i and 7j) are preserved in some medium-fine grained sandstone blocks that are similar to the sandstones from the

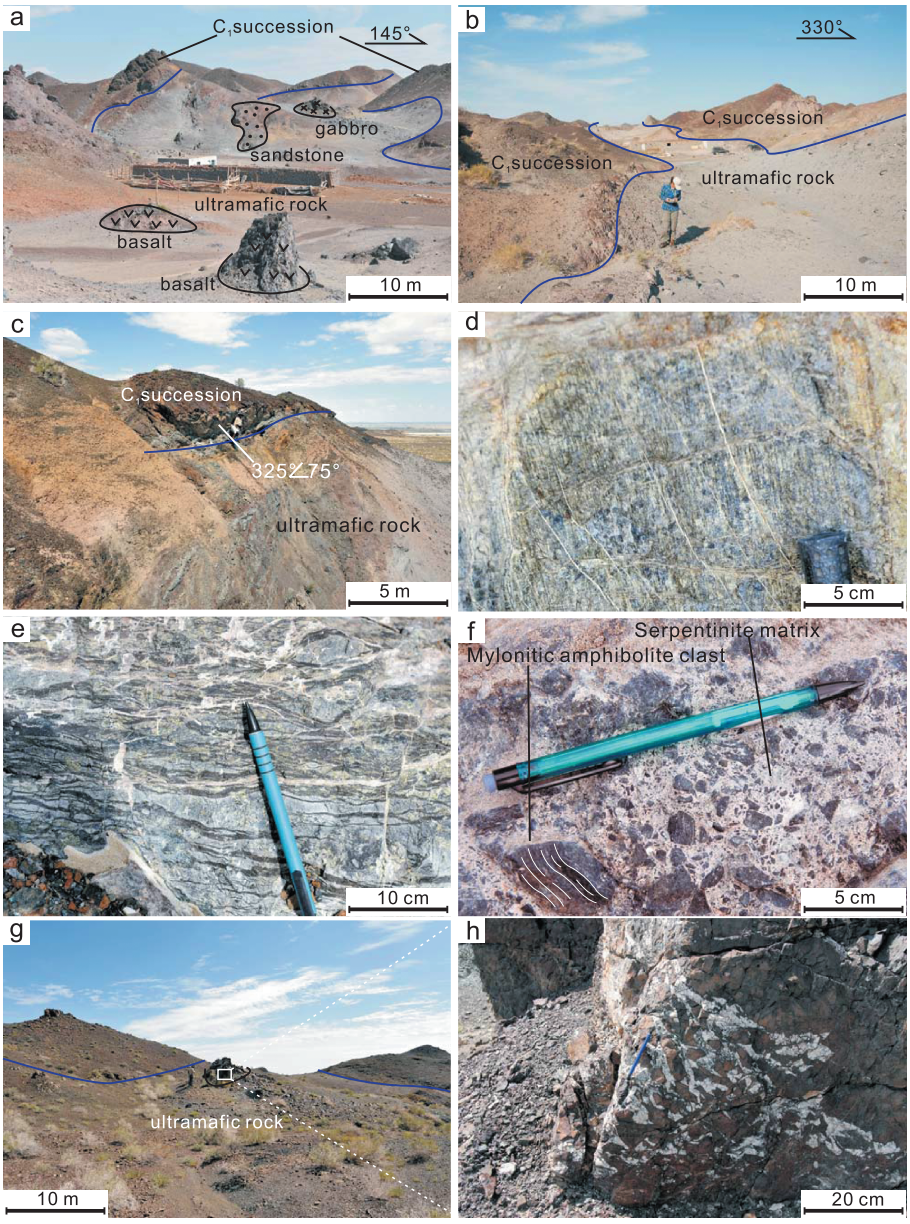

Figure 7. Field relationships and lithologies of the mélanges. (a) Serpentinized and foliated ultramafic rocks, with gabbro, sandstone, basalt showing block-in-matrix structures in the Baijiantan mélange. (b) Foliated serpentinite outcropping along steeply dipping fault in the Baijiantan mélange. (c) Serpentinized and foliated ultramafic rocks showing high-angle fault contact with the surrounding Carboniferous (C_1) basin-fill succession in the Baijiantan mélange. (d) Mylonitic peridotite block from the Baijiantan mélange. (e) Strongly foliated peridotite block from the Baijiantan mélange. (f) Amphibolite breccias consisting of mylonitic amphibolite clasts embedded within a serpentinite matrix of the Baijiantan mélange. (g–h) Block of peperitic basalt within the mélange. (i–j) Sandstone block within the mélange showing lenticular bedding. (k–l) Highly deformed and foliated tuffaceous conglomerate within the mélange. (m) Outcrop of the Darbut mélange showing block-in-matrix structures. (n) Subvertical planar fault contact plane of ultramafic rocks with Carboniferous (C_1) succession in the Darbut mélange.

Baogutu Formation. The lithologies of gravel clasts in some highly deformed and foliated tuffaceous conglomerates (Figures 7k and 7l) in the ophiolitic belt are identical with the lithologies of clasts in the tuffaceous conglomerates within the regional Xibeikulasi Formation [*Chen et al.*, 2013].

4.2. Darbut Ophiolitic Mélange

The Darbut ophiolitic mélange (outcrops approximately 105 km long and <5 km wide), is 40 km to the northwest and subparallel to the Baijiantan ophiolitic mélange, extending along the north side of the left-slip

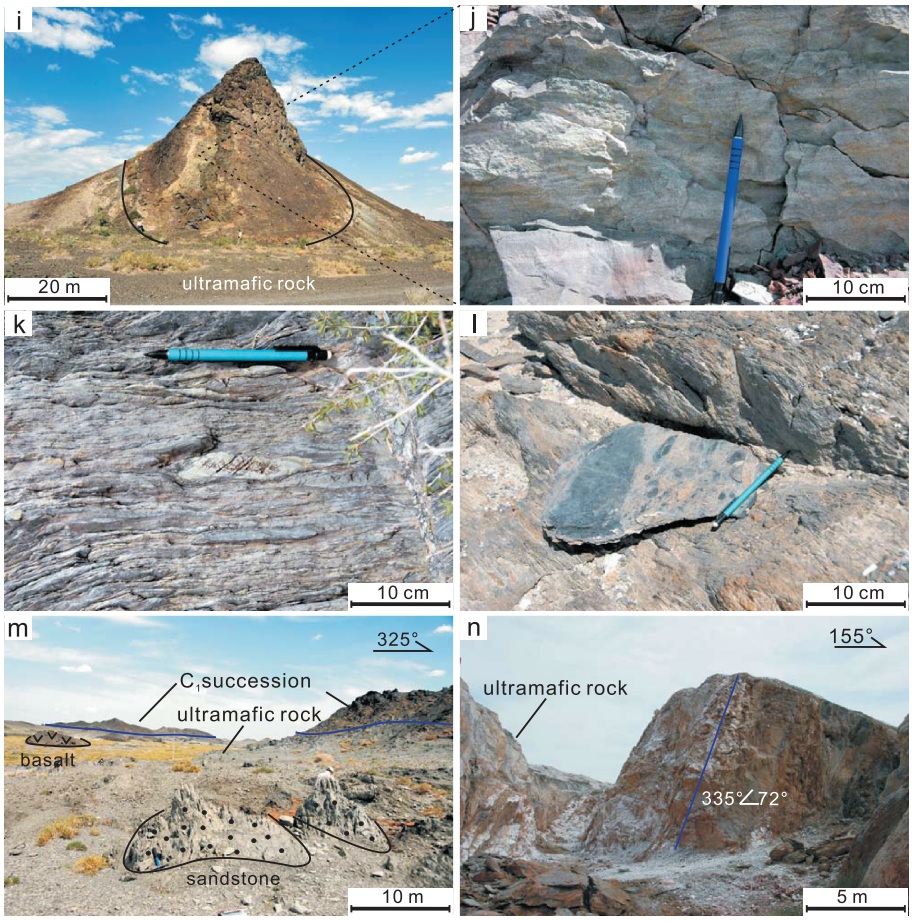

Figure 7. (continued)

Darbut Fault, striking NW (Figure 6). About 10 tectonic slices of mélange are distributed along a 100 km portion of the fault. However, the trend of the Darbut mélange is not controlled by the Darbut fault and the strikes of the eastern and western segments of the Darbut ophiolitic belt are distinctly different from the Darbut fault (Figure 6). Harzburgite and dunite tectonites have been serpentinized and highly sheared to form a flaky matrix of the mélanges that generally have steeply north-dipping fault contacts with the surrounding Carboniferous rocks (Figures 7m and 7n). Harzburgite, lherzolite, dunite, chromitite, troctolite, gabbro, basalt, tuff, sandstone, chert, and minor limestones occur as blocks within the serpentinite mélange. In Saertuohai, some highly deformed blocks of tuffaceous conglomerates are similar to fluvial conglomerate from the Xibeikulasi Formation at the top of the Carboniferous succession [*Chen et al*., 2013]. Most gabbro blocks are metasomatized to rodingite. The Darbut ophiolitic mélange has similar rock assemblages and structural features to the Baijiantan ophiolitic. A 50 m thick peperite-bearing succession containing pillow lava, radiolarian chert, fossiliferous limestones, and clastic sedimentary rocks was deformed and is in fault contact with serpentinized ultramafic rocks at Saertuohai (Figure 6).

5. Structural Patterns

The Baijiantan and Darbut ophiolites are both steep fault zones of serpentinite mélange that have classic structural features of left-slip shearing regimes recorded at the microscale to macroscale. Typical shear sense indicators have been identified in both mélanges.

Slip-fiber lineations. Slip-fiber lineations [*van der Pluijm and Marshak*, 1997] are the common expressions of slickenside lineations, produced by the preferred directional growth of minerals during the faulting and in the direction of movement, so that the plunge of the crystal fibers relative to the fracture surface reveals the

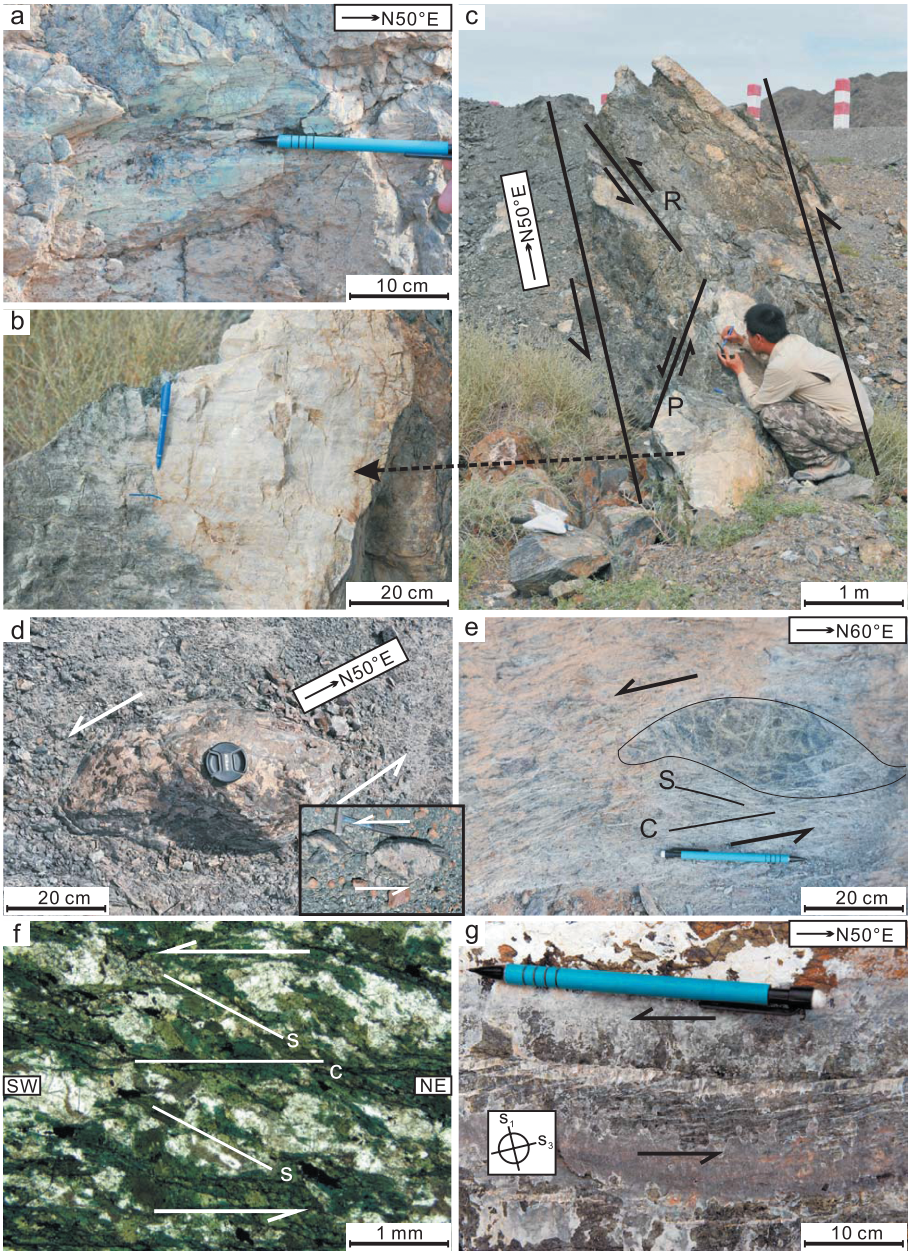

Figure 8. Photographs and photomicrographs of the structures associated with left-slip shearing within the mélange. (a) Vertical fault plane exhibiting subhorizontal slip fibers of serpentine. (b) Subhorizontal slip-fiber lineations on the thrust shear (*P*) plane. (c) Deformed block with Riedel (R) and Thrust shear (P) fissures. (d) Sigmoidal sheared block. Inset: sigmoidal blocks showing an en echelon arrangement. (e) *S-C* fabrics and sigmoidal peridotite block. (f) Oriented thin section of a mylonitic gabbro block: flattened and stretched hornblende and plagioclase grains displaying an *S-C* fabric. (g) En echelon arranged serpentine veins in a peridotite block.

sense of shear. The slickenside lineations in the mélanges are generally subhorizontal (<20°), striking east-northeast (Figures 5 and 6). On the subvertical fault contacts (>70°) of serpentinite matrix with surrounding Lower Carboniferous rocks of the Darbut and Baijiantan ophiolitic mélanges, typical slip-fiber lineation is well developed in serpentine (Figure 8a). The tiny microcliff escarpments all face the same direction, showing a left-slip sense of shear.

Riedel shears. Riedel shears, which are characteristic of strike-slip faulting [*Sylvester*, 1988], commonly occur within the blocks of the Darbut and Baijiantan ophiolitic mélanges. Generally, the blocks are dismembered by

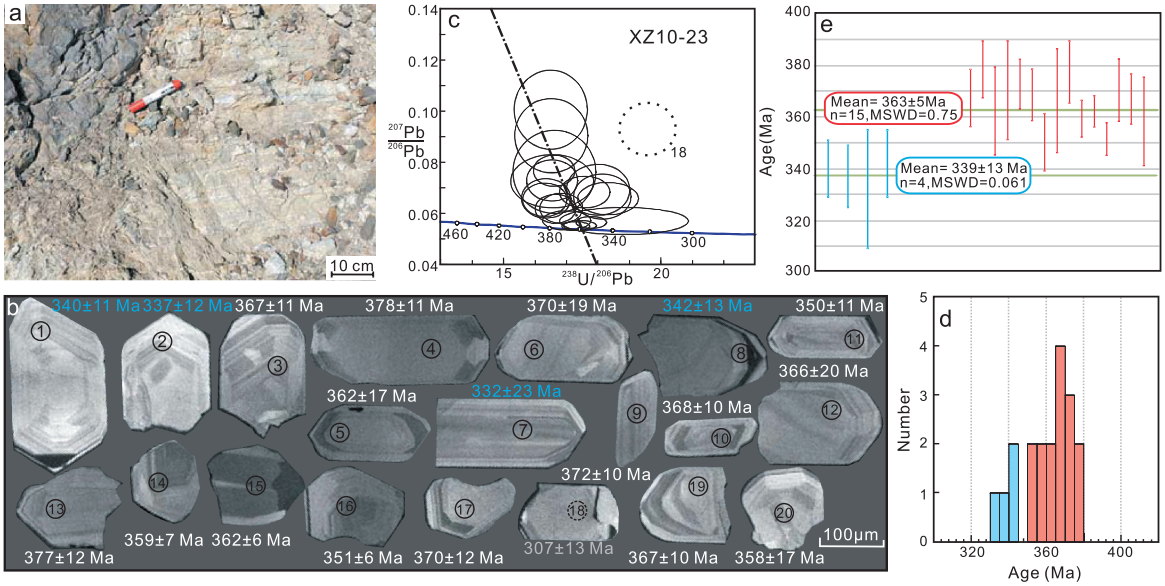

Figure 9. (a) Field outcrop of the cumulate gabbro sample (XZ10-23) in the Baijiantan ophiolitic mélange and (b) cathodoluminescence (CL) images of analyzed zircons in sample XZ10-23, (c) $^{207}Pb/^{206}Pb$-$^{238}U/^{206}Pb$ Tera-Wasserburg plot of SHRIMP U-Pb zircon dating, (d) frequency histograms, and (e) weighted average of $^{206}Pb/^{238}U$ ages for sample XZ10-23. Different colors of labels in Figure 9b indicate different groups.

two sets of steep secondary faults (Figure 8c), with left-slip kinematics revealed by the slip-fiber lineations (Figure 8b). One set is developed along N30°–40°E, at an acute angle to the main line of faulting (N50°E), corresponding to the Riedel shears. The other set, along the N70°–80°E direction, represents the synthetic shears known as *P* shears.

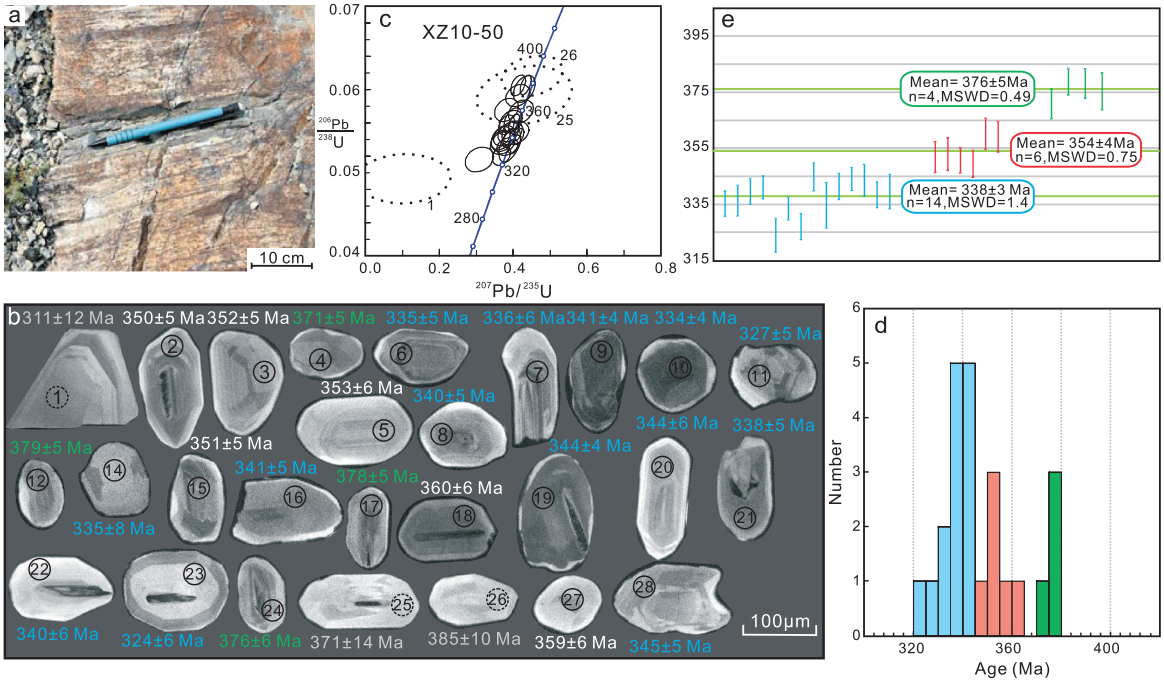

Figure 10. (a) Field outcrop of the cumulate gabbro sample (XZ10-50) in the Darbut ophiolitic mélange and (b) cathodoluminescence (CL) images of analyzed zircons in sample XZ10-50, (c) U-Pb concordia diagrams of zircons, (d) frequency histograms, and (e) weighted average of $^{206}Pb/^{238}U$ ages for sample XZ10-50. Different colors of labels in Figure 10b indicate different groups.

Asymmetric Blocks. Blocks within the mélanges on all scales generally have elongated shapes on horizontal surfaces and parallel alignments to the shear zone, which shows the subvertical polished surfaces with subhorizontal slickenside lineations (Figures 5 and 6). The relatively strong blocks responded to the deformation in a more rigid manner than the surrounding, ductilely deformed serpentinite matrix, whose shape and behavior should reflect the overall shear sense of the zone. The sigmoidal and lozenge shapes of centimeter- to meter- scale blocks are characteristic of left-slip shearing (Figure 8d). Several sigmoidal blocks show an en echelon arrangement expected from left-slip shearing (Figure 8d inset).

Shear Band Cleavages. Shear band cleavages generally develop as *S-C* fabrics as in granitic mylonites, which are among the most useful sense-of-shear indicators in ductile shear zones [*Berthé et al*., 1979; *Simpson and Schmid*, 1983]. Foliation in the serpentinite matrix anastomoses around lenses of blocks on all scales and is statistically planar, striking northeast-southwest and dipping steeply (Figures 5 and 6). On horizontal surfaces, the *S-C* fabrics consist of two foliations in the matrix as well as the sigmoidal peridotite blocks indicating left-slip shearing (Figure 8e). A few small blocks of gabbros are highly deformed and mylonitic, containing flattened and stretched hornblende and plagioclase grains showing an *S-C* fabric. Microscopic examination of the oriented thin sections (*XZ* plane) shows that the trace of the *C* planes has curved trajectories, and the *S* planes, defined by flattened and stretched hornblende and plagioclase, are oblique to the *C* plane shear band cleavages, again indicating a left-slip shear sense (Figure 8f).

Veins. Veins can be reliable shear sense indicators because their initial orientations are commonly controlled by the instantaneous stretching axes. In the peridotite blocks of the Baijiantan and Darbut ophiolitic mélanges, en echelon serpentine veins demonstrate a left-slip shearing (Figure 8g). The veins are oriented perpendicular to the axis of the maximum instantaneous extension (S_1), because this is the direction in which tension fractures form. The serpentine fibers grow in parallel to the S_1 via a crack-seal mechanism: a small increment of extension fracturing and the opening of the veins are followed by the growth of fibers from the existing crystals along the walls of the fracture [*Ramsay*, 1980].

6. Geochronology

6.1. Zircon SHRIMP U-Pb Dating of Gabbro

Zircon SHRIMP U-Pb dating was performed on a cumulate gabbro sample (XZ10-23) from a block of Baijiantan ophiolitic mélange (Figure 9a). The gabbro consists of plagioclase (50%), clinopyroxene (40%), amphibole (5%), and minor accessory minerals. Zircons are subhedral and irregularly shaped grains 100–250 μm long (Figure 9b). Most grains appear to have a core, with a break in growth pattern or zoning. Some cores have igneous zoning, others appear homogenous. Igneous zoned rims displaying oscillatory zoning are present in all grains except seven. Some of the analyzed grains are colorless and all have low U contents, leading to low concentrations of radiogenic Pb (Table 1). The ages for zircons are derived from the $^{206}Pb/^{238}U$ ratios, following correction for common Pb by the ^{207}Pb method [*Compston et al*., 1984] and results are displayed in Figure 9c as $^{207}Pb/^{206}Pb$-$^{238}U/^{206}Pb$ Tera-Wasserburg plots. Of 20 analyzed grains, one (spot 18) is highly discordant with significant Pb loss with a $^{206}Pb/^{238}U$ age at 307 Ma. Fifteen of the remaining spots located in cores of the grains have $^{206}Pb/^{238}U$ ages between 350 and 377 Ma with a weighted mean $^{206}Pb/^{238}U$ age of 363 ± 5 Ma (mean square weighted deviate (MSWD) = 0.75) (Figures 9d and 9e). The remaining three spots (spots 1, 2, and 8) located in the igneous zoned rims plus spot 7 (an entirely igneous zircon) have $^{206}Pb/^{238U}$ ages between 332 and 342 Ma with an average at 339 ± 13 Ma (MSWD = 0.061) (Figures 9d and 9e).

A cumulate gabbro sample (XZ10-50) from a block of Darbut ophiolitic mélange was also taken for zircon SHRIMP dating (Figure 10a) (Table 2). Zircons are granular with average length of 70–150 μm. Most zircons show wide growth zoning with a rim that is unzoned and bright in cathodoluminescence (CL) imaging. Some of the zircons are rather homogeneously bright in CL imaging, in some cases with a small dark core (Figure 10b). The ages for zircons are derived from the $^{206}Pb/^{238}U$ ratios, following correction for common Pb by the ^{204}Pb method and results are displayed in U-Pb concordia diagram (Figure 10c). In all 28 analyzed grains, one (spot 13) with a $^{206}Pb/^{238}U$ age at 77 Ma and another one (spot 1) with a $^{206}Pb/^{238}U$ age at 311 Ma are highly discordant with significant Pb loss. Two grains (spots 25 and 26) have high errors (>10 Ma). These four outliers are excluded in the calculation. The remaining 24 grains can be divided into three groups (Figure 10d): four of them have $^{206}Pb/^{238}U$ ages between 371 and 379 Ma with a weighted mean $^{206}Pb/^{238}U$

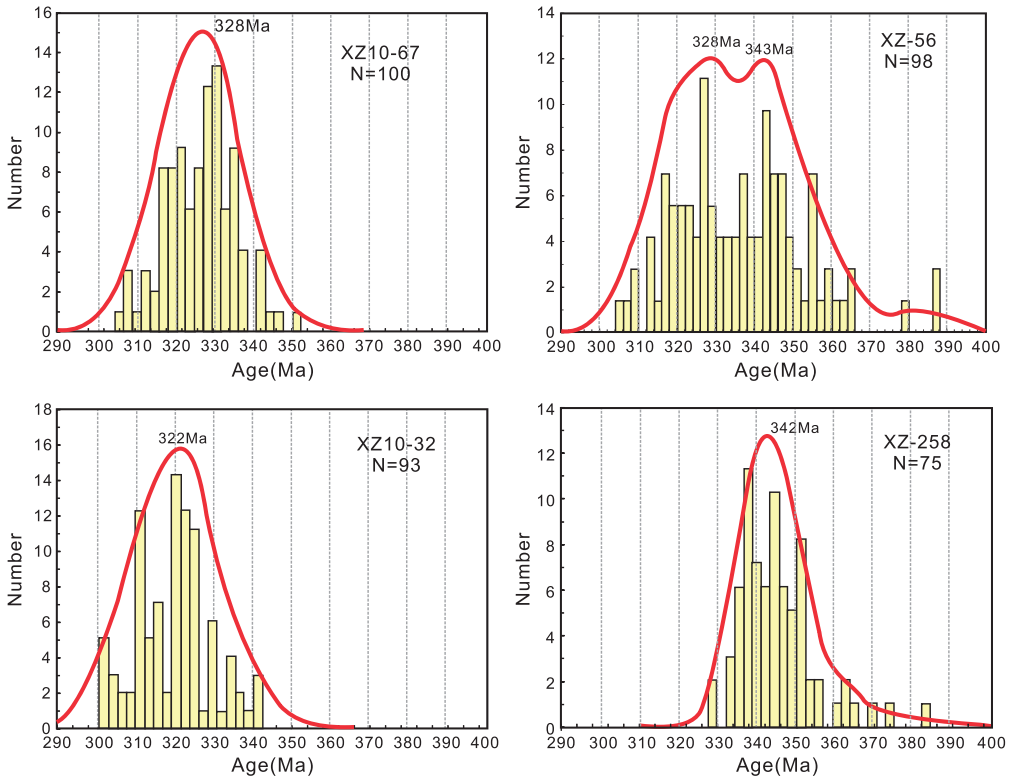

Figure 11. Age distributions of the detrital zircon U-Pb LA-ICP-MS dates of three sandstone blocks in the Baijiantan mélange (XZ10-67, XZ-56, and XZ10-32) and one sandstone sample from Carboniferous Xibeikulasi Formation (XZ-258).

age of 376 ± 5 Ma (MSWD = 0.49); six of them have $^{206}Pb/^{238}U$ ages between 350 and 360 Ma with a weighted mean $^{206}Pb/^{238}U$ age of 354 ± 4 Ma (MSWD = 0.75) and the remaining 14 spots have $^{206}Pb/^{238U}$ ages between 324 and 345 Ma with an average at 338 ± 3 Ma (MSWD = 1.4) (Figure 10e).

Although additional gabbro blocks were examined for zircon geochronology, they yielded either too few or no zircon grains. It is only in the cumulate gabbros that contain sufficient zircons for geochronological analysis.

6.2. Detrital Zircon LA-ICP-MS Dating of Sandstones

One sandstone sample (XZ-258) from the Carboniferous Xibeikulasi Formation and three sandstone samples (XZ10-67, XZ-56, and XZ10-32) from three different blocks within the Baijiantan ophiolitic mélange were selected to perform U-Pb detrital zircon LA-ICP-MS dating. Lithologies of these sandstones are similar, with dominant quartz and clay minerals, but many feldspars and lithic clasts are also preserved. Detrital zircon grains are generally euhedral and show oscillatory zoning on CL images, implying a magmatic origin. All the samples display a unimodal age distribution with an age range from 300 Ma to 390 Ma and a peak between 320 Ma and 350 Ma (Figure 11). The sample from the Lower Carboniferous Xibeikulasi Formation (XZ-258) yielded a cluster at 342 Ma and the youngest detrital zircon $^{206}Pb/^{238}U$ age is 330 Ma. The remaining samples are from blocks in the Baijiantan ophiolitic mélange. Both samples XZ10-67 and XZ10-32 have a single peak in the age spectrum at 328 Ma and 322 Ma, respectively. Sample XZ-56 shows a prominent peak around 320–350 Ma with clusters at 328 Ma and 344 Ma.

7. Discussion

7.1. The Significance of the Geochronological Data

The gabbro block from the Baijiantan ophiolitic mélange shows igneous cores of 363 ± 5 Ma and igneous rims of 339 ± 13 Ma. The age distribution in the gabbro block from the Darbut ophiolitic mélange has age clusters at 376 ± 5 Ma, 354 ± 4 Ma, and 338 ± 3 Ma. Other dates in the literature were also obtained from gabbro blocks from the Baijiantan and Darbut ophiolitic mélanges (Table 3). The data taken together imply prolonged mafic

Table 3. Summarized Geochronology Data of Igneous, Pyroclastic, and Clastic Rocks From West Junggar

Locality	Lithology	Age (Ma)	Method	Reference	Notes
Baijiantan mélange	Gabbro	363 ± 5	SHRIMP zircon U-Pb	This study	Obtained from one block
		339 ± 13			
		414 ± 9		*Xu et al.* [2006b]	Obtained from one block
		332 ± 14			
Darbut mélange	Gabbro	376 ± 5	SHRIMP zircon U-Pb	This study	Obtained from one block
		354 ± 4			
		338 ± 3			
		395 ± 12	Sm-Nd isochron	*Zhang and Huang* [1992]	
		391 ± 6	LA-ICP-MS zircon U-Pb	*Gu et al.* [2009]; *Yang et al.* [2012a]	N-MORB-like composition
		368 ± 11		*Yang et al.* [2012b]	Discordant data
Blocks in Baijiantan mélange	Sandstone	Range: 300–360 Mode: 328	LA-ICP-MS zircon U-Pb	This study	
		Range: 300–390 Mode: 328, 343			
		Range: 300–350 Mode: 322			
Xibeikulasi Formation		Range: 330–390 Mode: 342			
C succession in Baijiantan		Range: 300–410 Mode: ~330		*Zhang et al.* [2011a]	
C succession in Saertuohai		Range: 300–410 Mode: ~320		*Choulet et al.* [2012a]	
C succession in east of Akebastaw		Range: 300–460 Mode: ~320, ~420		*Choulet et al.* [2012c]	
Xibeikulasi Formation	Tuff	336 ± 3		*Guo et al.* [2010]	
Baogutu Formation	Tuff	342 ± 4–328 ± 4		*An and Zhu* [2009]	
	Andesite	345 ± 6		*Tong et al.* [2009]	
Tailegula Formation	Tuff	358 ± 5		*Guo et al.* [2010]	
	Tuff	364 ± 2		*Chen et al.* [2013]	Tuff lens enclosed by peperitic lava
Darbut mélange	Basalt	375 ± 2		*Yang et al.* [2012b]	OIB-like composition

magmatism throughout the Late Devonian and much of the Carboniferous recorded in single rock samples from the two ophiolitic belts. The phase at ~360 Ma correlates with peperite volcanism and the younger phase at ~330–340 Ma is of similar age to younger volcanic and pyroclastic rocks in the Carboniferous succession (Figure 12).

The three dated sandstone blocks from the Baijiantan ophiolitic mélange have a zircon assemblage with an age cluster in the range of 320–330 Ma (Figures 11 and 12). This is slightly younger than the cluster for the one dated sandstone sample from the Xibeikulasi Formation (342 Ma). The youngest dated tuff in the Xibeikulasi Formation was dated at 336 ± 3 Ma [*Guo et al.*, 2010] and is overlain by >1000 m of younger strata. The youngest detrital zircons in the sandstones are 307 ± 7 [*Choulet et al.*, 2012a], almost as young as the cross cutting ~302 Ma granitoid plutons. The three dated sandstone blocks thus appear to be from the middle part of the Xibeikulasi Formation. There is, however, evidence of tectonic incorporation of older rocks. These include lavas with associated chert containing Devonian radiolarian fossils [*Feng et al.*, 1989] and peperitic lavas (~364 Ma) derived from the base of the Carboniferous succession [*Chen et al.*, 2013]. The timing of the incorporation of these older rocks in the mélange is unknown. The samples from Baijiantan mélanges also have similar age distributions with sandstone samples from the Carboniferous succession in Saertuohai (DJ155) [*Choulet et al.*, 2012a], east of Akebastaw granite (DJ15) [*Choulet et al.*, 2012c], and Baijiantan (08YY02) [*Zhang et al.*, 2011a] (Table 3) (Figure 12). The sandstone blocks in the mélange thus come from the adjacent coeval basin fill. They are not exotic blocks transported by obducting crust in a conventional ophiolitic mélange.

7.2. Deformation and Metamorphism of the Ophiolitic Mélanges

The Baijiantan and Darbut mélanges share many diagnostic key features with mélanges related to strike-slip tectonics (Figures 5–8) [*Orange*, 1990; *Festa et al.*, 2010], which include steeply dipping fault contacts (>70°)

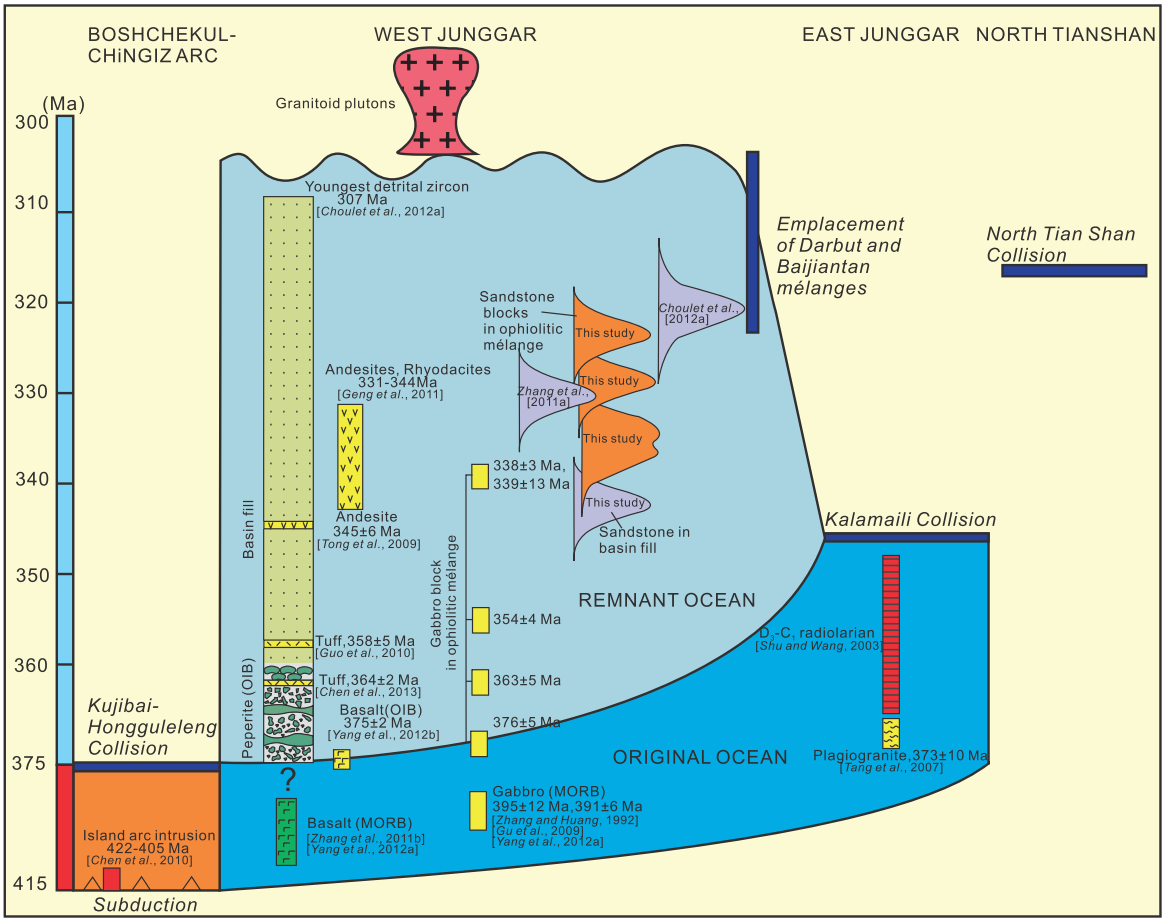

Figure 12. Cartoon showing chronologic control for magmatism and tectonic evolution of West Junggar and surrounding terranes. For details of geochronology, see Table 3.

and subhorizontal slickenside lineations (<20°), consistent and steeply dipping foliation (>75°) in the matrix, rare angular and elongated shape of the blocks and their parallel alignment to the shear zone, and microscale to macroscale classic structural features of strike-slip regimes (e.g., *S-C*, Riedel shears, scaly cleavages). Consistent shear sense indicators within the mélanges including slip-fiber lineations, Riedel shears, asymmetric blocks, shear band cleavages, and veins indicate a horizontal left-slip sense of movement. In contrast to mélanges incorporated into an ophiolitic accretionary complex [*Kimura et al.*, 1996; *Kusky and Bradley*, 1999; *Polat and Kerrich*, 1999], typical imbricate structures, thrust duplexes, and thrust faults are absent. The Darbut and Baijiantan ophiolitic belts thus act as two parallel sinistral shear zones. The Carboniferous formations between Darbut and Baijiantan ophiolitic mélanges were folded, steepened, and developed into synclines in parallel with the belts (Figure 3), as a result of compressional action during the movement of the shear zones. The asymmetric S-shaped drag folds marked by deformed limestone lenses, sigmoidal shape limestone phacoids, horizontal mineral/stretching lineation, and asymmetric fold limbs in limestone near the Darbut mélange in Saertuohai, and folds with vertical axes in the Carboniferous rocks identified by *Choulet et al.* [2012a] indicate a sinistral shearing along a N50°E direction. These can be interpreted as expressions of Carboniferous ductile deformation related to movement on the Darbut and Baijiantan shear zones.

Some vertical motion is necessary within the strike-slip zones. Common large serpentinite and peridotite blocks are of mantle origin and require a mechanism to move them to upper crustal levels, even if the crust is thin (oceanic plus sediment fill). Deep structural discontinuities can provide a permeable pathway resulting in high water-rock ratios at upper mantle depths, which facilitates serpentinization. If the serpentinization proceeds far enough to yield a significant density differential, protrusive activity may commence along the pathways [*Bonatti*, 1976, 1978; *Saleeby*, 1984]. However, the mechanism for uplift of mantle peridotite and serpentinite in modern oceanic fracture zones remains an issue of debate [*Campos et al.*, 2010].

Although volcanic rocks and gabbros in the mélanges are generally altered to greenschist or prehnite-pumpellyite facies, rare pods of amphibolite and mylonitic peridotite are present (Figures 7d–7f). Amphibolite breccias (Figure 7f) in the Baijiantan mélange contain sharp mylonitic amphibolite clasts, which are similar to fault rocks and indicate polyphase deformation history of the mélanges. *Angiboust et al.* [2012] identified eclogite breccias from the Monviso ophiolite in the Western Alps made of fragments of eclogite mylonite cemented by omphacite, lawsonite, and garnet that were later embedded in serpentinite, which were interpreted as resulting from an ancient fault zone associated with intraslab earthquakes. The similar amphibolite breccias in Baijiantan and the ultramafic mylonites probably record early, deep-seated strike slip or they might reflect intense deformation at the margins of deeper, hotter portions of a diapir that passed upward into serpentinite. The amphibolite-facies metamorphism then was superimposed at a shallow level to form amphibolite breccia during the mélange formation.

7.3. Timing of Deformation

Based on the structural pattern analysis, the Darbut and Baijiantan ophiolitic mélanges acted as two sinistral wrench shear zones which largely deformed under ductile and low-temperature rheological conditions. However, the deformation of the mélanges was polyphase, as demonstrated by the amphibolite breccias, and the starting time of the shear is uncertain.

The youngest units within the mélanges are the deformed blocks of Carboniferous basin-fill sedimentary rocks (Figures 7i–7l). The final deformation of the mélanges postdated the 322 Ma age cluster (Figure 11) of the incorporated sandstone blocks. The youngest age in the gabbro sample of ~338 Ma indicates that the gabbros could have been incorporated in the mélange a little earlier. The termination of deformation is dated by the stitching alkaline granitoid plutons and related dikes, which have modal age of ~302 Ma [*Han et al.*, 2006; *Geng et al.*, 2009; *Chen and Guo*, 2010; *Zhang et al.*, 2011a] (Figure 6). The ultimate formation of the mélanges is thus constrained between 322 Ma and ~302 Ma (Figure 12).

Younger deformation was taken up on the transcurrent left-slip Darbut Fault (Figures 3 and 6) [*Allen et al.*, 1995; *Choulet et al.*, 2012a]. This deformation is characterized by brittle deformations (such as steep fault scarps and brittle fault rocks) and probably started in Permian time, since the Upper Permian conglomerates occurring along the fault valley provide the evidence of syntectonic sedimentation [*Allen et al.*, 1995]. The elongated characteristics and the offset of the Upper Carboniferous Keramay granitoid pluton (301 ± 5 Ma) [*Han et al.*, 2006] results from the Yijiaren Fault, a splay of the Darbut Fault (Figure 3). The Paleogene Ulunguhe Formation in the Hoxtolgay area was dislocated by the Darbut Fault, indicating significant sinistral displacement in the Cenozoic [*Xu et al.*, 2009; *Meng et al.*, 2009].

7.4. A Strike-Slip Fault Zone Origin of the Ophiolitic Mélanges in a Continuous Ocean Basin

Previous authors have considered West Junggar to represent some form of subduction-accretion complex, as reviewed in section 2 above and summarized in Figure 4. The characteristic upright fold hinges, imbricate structures and thrusts formed in an accretionary complex are rarely observed in West Junggar, although the bedding of the formations generally dips steeply. Between the Baijiantan and Darbut ophiolitic belts, the Tailegula, Baogutu, and Xibeikulasi formations form synclines that parallel the belts and the formations trend mainly in a north-south direction (Figure 3). There is no evidence that the Darbut ophiolitic mélange separates two different terranes. The similarity of lithologies of the sediments in both NW and SE sides of Darbut ophiolitic mélange was already recognized by *BGMRXUAR* [1966] and confirmed by available geochronological data of pyroclastic rocks and sandstones from stratigraphic units on either side of the Darbut fault (Figure 12) (Table 3). In addition to the similarity of the Carboniferous sediments around the Darbut and Baijiantan ophiolitic belts, the peperitic basaltic lavas (circa 364 Ma) and the interbedded and overlying sedimentary rocks form a continuous stratigraphic section at the bottom of the Carboniferous successions [*Chen et al.*, 2013], which is distributed regionally with variable strike over a distance of 100 km (Figure 3) and varies little on either side of the Darbut and Baijiantan ophiolitic mélanges (Figures 5 and 6). The peperite-bearing units display complete cycles of volcanism formed by in situ reaction between basaltic lava and unconsolidated marine sediments [*Chen et al.*, 2013], which distinguishes them from tectonic slices in an ophiolitic accretionary complex. Peperites at the bottom of the Carboniferous strata with OIB geochemical features [*Zhu et al.*, 2007; *Zhang et al.*, 2011b] was formed in the ocean basin in the Late Devonian, representing the upper components of the ocean crust [*Chen et al.*, 2013]. Therefore, they are

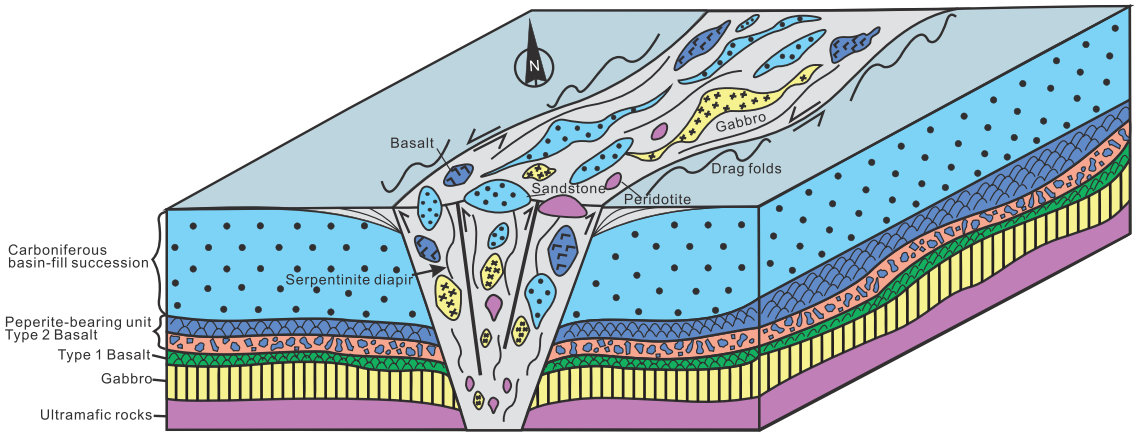

Figure 13. Schematic diagram showing the oceanic crust, ocean basin-fill, fault zones, and serpentinite mélange in West Junggar (not to scale).

marker layers of the uppermost ocean crust to signify that the Darbut and Baijiantan regions were covered by a continuous ocean basin in Late Devonian during extrusion of the peperitic flows. Late Carboniferous rock assemblage of 321–305 Ma ore-bearing porphyries with adakitic characteristics and high-Mg diorite dykes [*Jin and Zhang*, 1993; *Liu et al*., 2009; *Geng et al*., 2009; *Tang et al*., 2010; *Yin et al*., 2010] were reported, which are coeval with the stitching alkaline granitoid plutons [*Han et al*., 2006; *Chen and Guo*, 2010] (Figure 3). However, there are no significant Late Devonian to Early Carboniferous arc-signature rocks in this region that would be expected from the previously proposed subduction and accretionary process.

All of the above evidence is not consistent with an origin of an accretionary complex associated with the ophiolitic belts. The Darbut and Baijiantan ophiolitic belts appear to be crustal-scale tectonic lineaments in a continuous ocean basin, bringing up slices of oceanic crust and upper mantle. They cannot be interpreted as evidence of significant plate boundaries or subduction suture zones in the Devonian to Carboniferous and are thus distinct from the other ophiolitic belts in North Xinjiang that generally separate different terranes (Figure 2).

The Darbut and Baijiantan belts acted as two parallel left-slip fault zones containing ophiolitic materials. Similar cases of fault zones involving ophiolitic material, but not marking plate sutures, have been identified elsewhere. The Irtysh (also called Ertix, Irtysh, Erqis, or Erqishi) suture zone between the Altai arc and the Early Carboniferous Zharma-Saur arc and Dulate-Baytag arc in Chinese Altai has been has been modified by Irtysh thrust fault, along which the Paleozoic Irtysh mélange complex was exhumed to the upper crust at circa 280 Ma [*Briggs et al*., 2007, 2009]. The Cenozoic strike-slip Kunlun fault in central Tibet reactivated the Triassic Anyimaqen-Kunlun-Muztagh suture zone [*Yin and Harrison*, 2000] and contains ophiolitic materials in many places but has nothing to do with the closure of the paleo-Tethys ocean. In the Chinese Qilian Shan region, the Cenozoic Qilian-Nan Shan imbricate thrust belts brought up and duplicated the Devonian Qilian mélange complex formed during the collision between the Qilian arc and North China, which produced apparently multiple suture zones [*Yin et al*., 2007]. A similar case was also reported in the Bangong-Nujiang suture zone in western Tibet [*Kapp et al*., 2003].

In contrast, in West Junggar the ophiolitic mélanges were not reactivated from older ophiolitic successions, since the young ages of included gabbro blocks compared with that on the surrounding sedimentary succession (and its included blocks) indicates that deformation is essentially synchronous with igneous activity. The Meso-Cenozoic Darbut strike-slip faulting show shallow, brittle characteristic of deformation, which has different trend and extent of deformation and has no connection with the Darbut ophiolitic mélange (Figures 3 and 6). In Baijiantan area, Paleozoic formations and mélange is unconformably overlain by approximately horizontal Mesozoic strata indicate that there is no apparently later structural reworking in Baijiantan ophiolitic mélange (Figure 3). The strike-slip faulting involving the Darbut and Baijiantan ophiolitic mélanges was developed within oceanic crust, as indicated by the regional development of Devonian peperitic lavas and the occurrence of the amphibolite and ultramafic mylonite in the mélanges. The lithologies of the ophiolitic mélanges include ultramafic rocks (indicative of upper mantle), gabbro, MORB-like basalt, OIB-like peperitic basalt (representing oceanic crust), and sedimentary rocks that

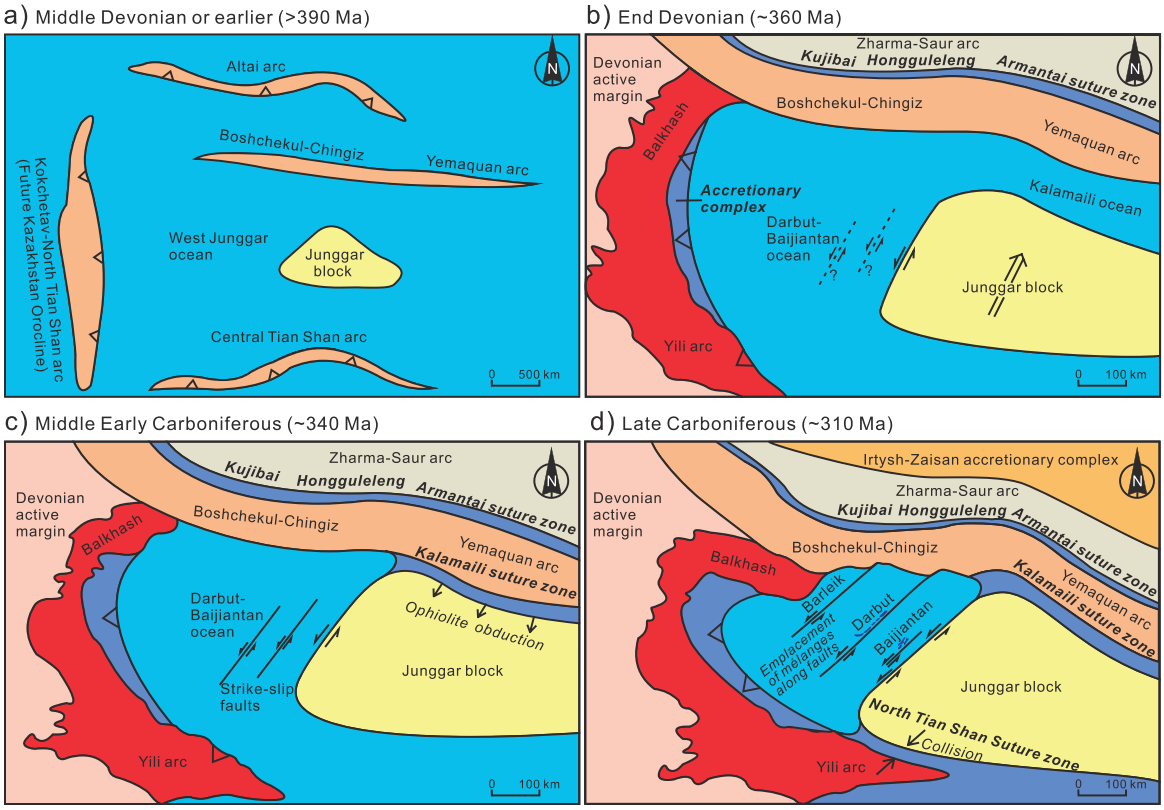

Figure 14. Diagrams illustrating the tectonic evolution of the West Junggar and surrounding terranes from the Middle Devonian to the Late Carboniferous. (a) North Xinjiang and surrounding area made up an archipelago paleogeography in Paleozoic. The ocean in West Junggar was in connection with other ocean as a normal spreading ocean basin. (b) Subduction ended in the paleo-ocean basin represented by the Honggueleng-Kujibai-Armantai ophiolite belt by Late Devonian and the bending of the Balkhash-Yili arc started. The oceanic basin in West Junggar started to receive sufficient sediment deposition into which basalts flows could bulldoze to form the regional distributed peperites (c) Collision took place between the Junggar block and the Yemaquan arc with further bend of the Balkhash-Yili arc in Early Carboniferous and a remnant ocean basin was preserved in West Junggar. The relative motion between Junggar block and ocean basin caused NW trending left-slip fault zones within the remnant ocean basin. (d) Reactivation of the strike-slip faults resulting from the docking of the Yili arc with the Junggar block in the Late Carboniferous and the accomplishment of the oroclinal bending of the Balkhash-Yili arc finally facilitated the emplacement of the Baijiantan and Darbut ophiolitic mélanges.

resemble the surrounding sediments in lithology and age (Figures 7d–7l). The Baijiantan and Darbut ophiolitic mélanges thus are autochthonous and consist of locally derived rocks that distinguish them from conventional ophiolitic mélanges as representative of suture zones (Figure 12). They originated as crustal-scale left-slip fault zones in an ocean basin. Tectonically disrupted mafic oceanic crust and basin-fill sediments, as well as the ultramafic protrusions along the fault zones make up the mélanges (Figure 13).

The clusters in zircon ages from the cumulate gabbros at ~375, ~360, ~354, and ~340 Ma imply episodic supply of new magma from the mantle into a magma chamber within the stability field of plagioclase and amphibole, probably within the lower crust. Each new magma pulse remobilized crystal mush cumulates in a long-lived magma chamber [as inferred by *Brown et al.*, 1998]. The episodic supply of magma is also reflected in the known ages of volcanic rocks: ~375 and ~360 Ma for the peperites [*Chen et al.*, 2013], ~354 Ma for a tuff [*Guo et al.*, 2010], and ~340 Ma for andesites, trachytes, and rhyodacites [*Tong et al.*, 2009; *Geng et al.*, 2011] (Figure 12). We can consider two hypotheses for such episodic magma supply. It may result from episodic processes in the mantle, changing either temperature or pressure to produce mafic magma by partial melting of ultramafic mantle. In this scenario, it is difficult to understand the persistence of a crustal magma chamber for at least 35 Ma. Alternatively, production and migration of melt in the mantle may be more continuous, but the availability of pathways through the crust is related to episodic movement along the strike-slip crustal-scale faults. In this scenario, magma chambers and overlying volcanoes were likely positioned at extensional offsets in strike-slip faults or at the intersection with other fault lineaments [e.g., *McNulty et al.*, 1998; *Acocella and Funiciello*, 2010; *Shabanian et al.*, 2012]. Episodic fault movement associated with regional collisional tectonics led to the localization of volcanism in time and space, the latter

indicated by variable thicknesses of peperites [*Chen et al*., 2013] and the presumed existence of discrete Early Carboniferous volcanoes in the West Junggar Basin. It is likely, but not proven, that the Darbut and Baijiantan shear zones that led to eventual ophiolite emplacement were reactivated from earlier transtensional shears that localized the long-lived magma chambers, in a manner analogous to that described from a different type of postcollisional setting in Iran by *Shabanian et al*. [2012].

7.5. Regional Plate Tectonic Evolution

7.5.1. Middle Devonian Spreading

It is widely accepted that there were multiple subduction zones that had an archipelago paleogeography similar to that in the present SW Pacific [*Xiao et al*., 2003, 2004a, 2004b, 2008; *Windley et al*., 2007] during the Middle Paleozoic in the CAOB. The ocean in West Junggar was connected with other oceanic regions in North Xinjiang to form an extensive normal ocean basin in the Middle Devonian or earlier (Figure 14a).

7.5.2. Late Devonian to Late Carboniferous Collisions

The most important tectonic changes in North Xinjiang during the Late Devonian to Early Carboniferous were a series of collision events. The Ordovician Armantai ophiolite was emplaced onto mid-Devonian volcanic-sedimentary strata that were unconformably overlain by Lower Carboniferous strata in the Dulate-Baytag arc [*Zhang and Guo*, 2010]. The Hongguleleng and Kujibai ophiolites were partly covered by Lower Carboniferous molasse that contains various ophiolite fragments [*Zhu and Xu*, 2006]. The Hongguleleng ophiolite was also considered to be postdated by latest Ordovician conglomerate and unconformably covered by Silurian Sharbuert Formation [*Choulet et al*., 2012b]. Therefore, the Armantai-Hongguleleng-Kujibai suture zone is considered to have been formed prior to Early Carboniferous (Figures 12 and 14b).

The Kalamaili ophiolite in the east side of Junggar Basin has a plagiogranite age of 373 ± 10 Ma [*Tang et al*., 2007] and Late Devonian to Early Carboniferous (D_3–C_1) radiolarians [*Shu and Wang*, 2003]. The MORB ocean crust here is thus younger than that in the Baijiantan and Darbut ophiolites in West Junggar. Together, they appear to represent a Devonian paleo-ocean basin stretching across Northern Xinjiang (Figures 12 and 14b). It is generally accepted that the Kalamaili suture zone formed later than the Armantai suture zone [e.g., *Xiao et al*., 2008; *Han et al*., 2010]. The Kalamaili ophiolite is unconformably overlain by Lower Carboniferous strata [*Li*, 1995]. Ophiolitic-clast-bearing molasse deposits were deposited south of the Kalamaili ophiolitic belt as a consequence of the continental collision. The age of the molasse was constrained to be between 343.5 and 345 Ma [*Zhang et al*., 2013]. All this evidence demonstrates that the Kalamaili ophiolite was emplaced before the Visean (Figures 12 and 14c).

The collision between the Yili arc and Junggar block, defined by the youngest Bayingou ophiolite (plagiogranite age of 325 Ma by *Xu et al*. [2005] and a gabbro age of 344 Ma by *Xu et al*. [2006a]), postdated the Late Devonian Armantai- Hongguleleng- Kujibai collision and the Early Carboniferous Kalamaili collision. The stitching granite that intruded the Bayingou ophiolite has a zircon U-Pb age of 316 Ma [*Han et al*., 2010], indicating that the Junggar block and Yili arc collided in the Late Carboniferous (Figures 12 and 14d).

7.5.3. Late Devonian-Carboniferous Remnant Ocean Basin Deformed by Strike-Slip Fault Zones

The termination of N-MORB basalts and the onset of a plentiful supply of terrigenous sediments (Figure 12), which is consistent with regional Late Devonian to Early Carboniferous collision events, demonstrate the end of spreading in West Junggar region. The West Junggar region can be extended westward into the Kazakhstan orocline (Figure 1b). The palaeomagnetic data obtained in the segments of the orocline documented that since Late Devonian, the convergence of Tarim and Siberia caused a bending of the NW trending Devonian active margin [*Abrajevitch et al*., 2008] (Figure 1b). It is proposed that the oroclinal bending took place in the Devonian and Early Carboniferous and completed by the Late Carboniferous [*Levashova et al*., 2012], which is also consistent with regional Late Devonian to Early Carboniferous collisional events in North Xinjiang. The paleo-Junggar Ocean in the West Junggar area, situated in the easternmost inner part of the orocline, could not be completely closed during the bending of the Kazakhstan orocline, resulting from the resistance of the internal Junggar block and the protection from the special boundary condition which was reserved in the final closure of collision in adjacent Tianshan or Junggar (Figures 12 and 14). A remnant ocean basin preserved in West Junggar during the Late Devonian to Carboniferous (Figure 12) [*Chen et al*., 2013] is comparable with the modern Black Sea.

The Baijiantan and Darbut ophiolitic mélanges represent oceanic crust disrupted along two left-slip fault zones within the remnant ocean basin. The fault zones are NE trending and parallel to the western boundary

of the Junggar block. They differ from the northwest to west-northwest trending suture zones in North Xinjiang, indicating that they were associated with the relative motion between the Junggar block and West Junggar basin as a result of regional collisions (Figure 14).

The northeastward movement of the Junggar block and the resulting collision with the Yemaquan arc along the Kalamaili ophiolitic suture zone in Early Carboniferous would result in movement of the strike-slip fault zones and supply of magma, which is consisting with the cluster at ~340 Ma in zircon ages from the cumulate gabbros (Figures 12 and 14c). The amphibolite and ultramafic mylonites within the mélanges probably record this early shearing.

During the later part of the Early Carboniferous (~320 Ma), the oroclinal bending of the Balkhash-Yili arc completed and the remnant ocean basin was almost filled with sediment when the Baogutu Formation was deposited, because a shallow marine and littoral paleo-environment is indicated by the widespread developments of cross bedding, lenticular bedding, and coral fossils in this formation. The remnant basin had been deformed and shrunk in the regional compressional regime, as recorded by some locally preserved pre-strike-slip upright folds and thrusts identified in the Carboniferous succession [*Choulet et al*., 2012a; *Zhang et al*., 2011a]. Nevertheless, the distinction between the deformation in an earlier stage of compressive tectonics with the deformation related to movement along the transpressional Darbut and Baijiantan shear zones is difficult and unclear, such as the restricted occurrence of overturned folds and thrusts near the Baijiantan shear zone similar to a flower structure [*Zhang et al*., 2011a]. The collision of the Yili arc and Junggar block brought about further reactivation and transformation from transtension to transpression in the strike-slip fault zones, disrupting the oceanic crust and Carboniferous basin-fill successions and leading to diapiric emplacement of serpentinite to form the ophiolitic mélanges (Figures 12 and 14d). The brecciation of the amphibolite identified in the Baijiantan ophiolitic mélange probably formed during this reactivation, which resulted in the formation of the present style of the mélanges. Along with the movement of the crustal-scale strike-slip fault zones, the trapped oceanic crust was intensively deformed and destroyed, as evidenced by blocks of oceanic crust components within the mélanges and the steeply dipping bedding of the peperite-bearing successions [*Chen et al*., 2013]. Meanwhile, the basin-fill sediments were steepened, folded and thickened by stratigraphic repetition. Thereafter, juvenile silicic crust was emplaced, represented by the Late Carboniferous stitching plutons with strongly positive ε_{Nd}, marked the final closure of the remnant ocean basin. Subsequently, West Junggar was involved in the intracontinental setting, which facilitated the initiation of the Darbut Fault.

The subduction and closure of the ocean basin in West Junggar occurred in Early Paleozoic, as constrained by the emplacements of ophiolites, arc plutons, and blueschists in the Tangbale and Mayile areas [*Choulet et al*., 2012b; *Xu et al*., 2012; *Ren et al*., 2014; *Zhang*, 1997]. The Junggar Ocean was enclosed in the Kazakhstan orocline and subduction was active along the margins of the orocline, while accretionary wedge developed in Carboniferous (Figure 14) [*Choulet et al*., 2012a]. The final closure of paleo-oceanic Junggar basin occurred in the Darbut-Baijiantan area within the innermost Kazakhstan orocline, where an infilled remnant oceanic basin was preserved and deformed by crustal-scale strike-slip fault zones, resulting in emplacement of linear ophiolitic mélanges. Even though question remains as to the detailed kinematic mechanism for the geodynamic evolution of remnant oceanic basin, this inferred tectonic model of West Junggar in Paleozoic in good agreement with geological and structural data provide an important perspective for better understanding of Paleozoic evolution of West Junggar and the CAOB.

8. Conclusions

The Baijiantan and Darbut ophiolitic mélanges are examples of oceanic shear zones in a remnant ocean basin, with parallel steeply dipping fault zones bounding a foliated serpentinite matrix containing a range of deformed sedimentary and igneous blocks. They are in tectonic contact with regionally distributed Late Devonian-Early Carboniferous (D_3-C_1) ocean floor peperitic basalts and overlying deepwater Carboniferous sedimentary successions, from which the sedimentary blocks were derived.

Blocks of cumulate gabbro in the shear zones have multiple clusters of zircon ages, spanning tens of millions of years, with the oldest similar in age to the regional peperitic OIB basalts, but younger clusters synchronous with accumulation of the overlying Carboniferous sediments. Such age distributions are inconsistent with interpretation of the mélanges as an accretionary complex and imply continuing magmatism along the shear

zones. The ophiolitic mélanges are crustal-scale strike-slip fault zones in an ocean basin, not major plate boundaries nor subduction suture zones.

The remnant ocean basin was trapped following regional collisions and bending of Kazakhstan orocline during Late Devonian to Early Carboniferous. The sinistral fault zones are parallel to the western boundary of the Junggar block, indicating that they were associated with relative motion between the Junggar block and West Junggar ocean basin. Reactivation of the fault zones, resulting from the collision between the Yili arc and Junggar block accompanying with the accomplishment of the oroclinal bending in the Late Carboniferous disrupted the oceanic crust and basin-fill successions and caused diapirs of serpentinite under sinistral shear to finally emplace the Baijiantan and Darbut ophiolitic mélanges.

The remnant oceanic basin trapped in Late Devonian to Carboniferous in West Junggar was filled with several kilometers of Carboniferous sedimentary rocks. Widespread emplacement of upper crustal juvenile granitoids in the latest Carboniferous was probably accompanied by crustal thickening by the same magma deeper in the crust. Crustal-scale Permian strike-slip faults further obscured the original ocean basin.

Acknowledgments

This study is supported by a grant of the National Natural Sciences Foundation of China (41272239) and the National Science and Technology Major Project (2011ZX05009-001) to Z. Guo and Research Funds Provided to New Recruitments of China University of Petroleum-Beijing (2462013YJRC020) and the Foundation of State Key Laboratory of Petroleum Resources and Prospecting, China University of Petroleum (PRP/indep-4-1306) to S. Chen. We are grateful to Jinhai Yu for his suggestion on the manuscript. We gratefully acknowledge Tectonics Editors John Geissman and Todd Ehlers and Associate Editor Paul Kapp. We would like to thank An Yin, Wenjiao Xiao, and Dr. Flavien Choulet for constructive reviews.

References

Abrajevitch, A., R. Van der Voo, N. M. Levashova, and M. L. Bazhenov (2007), Paleomagnetic constraints on the paleogeography and oroclinal bending of the Devonian volcanic arc in Kazakhstan, *Tectonophysics*, *441*(1), 67–84, doi:10.1016/j.tecto.2007.04.008.

Abrajevitch, A., R. Van der Voo, M. L. Bazhenov, N. M. Levashova, and P. J. McCausland (2008), The role of the Kazakhstan orocline in the late Paleozoic amalgamation of Eurasia, *Tectonophysics*, *455*(1), 61–76, doi:10.1016/j.tecto.2008.05.006.

Acocella, V., and F. Funiciello (2010), Structural control of arc volcanism and related kinematic setting: An overview, *Earth Planet. Sci. Lett.*, *289*, 43–53, doi:10.1016/j.epsl.2009.10.027.

Allen, M. B., A. M. C. Şengör, and B. A. Natal'in (1995), Junggar, Turfan and Alakol basins as Late Permian to? Early Triassic extensional structures in a sinistral shear zone in the Altaid orogenic collage, Central Asia, *J. Geol. Soc.*, *152*(2), 327–338, doi:10.1144/gsjgs.152.2.0327.

An, F., and Y. F. Zhu (2009), SHRIMP U-Pb zircon ages of tuff in Baogutu Formation and their geological significances [in Chinese with English abstract], *Acta Petrol. Sin.*, *25*(6), 1437–1445.

Angiboust, S., P. Agard, P. Yamato, and H. Raimbourg (2012), Eclogite breccias in a subducted ophiolite: A record of intermediate-depth earthquakes?, *Geology*, *40*(8), 707–710, doi:10.1130/g32925.1.

Berthé, D., P. Choukroune, and P. Jegouzo (1979), Orthogneiss, mylonite and non coaxial deformation of granites: The example of the South Armorican Shear Zone, *J. Struct. Geol.*, *1*(1), 31–42, doi:10.1016/0191-8141(79)90019-1.

BGMRXUAR (Bureau of Geology and Mineral Resources of Xinjiang Uygur Autonomous Region) (1966), Introduction of geological map of Karamay area [in Chinese], *Map L-45-XIX scale at 1:200000*, Xinjiang Bureau of Geology and Mineral Resources, Xinjiang, China.

Bonatti, E. (1976), Serpentinite protrusions in the oceanic crust, *Earth Planet. Sci. Lett.*, *32*(2), 107–113, doi:10.1016/0012-821X(76)90048-0.

Bonatti, E. (1978), Vertical tectonism in oceanic fracture zones, *Earth Planet. Sci. Lett.*, *37*(3), 369–379, doi:10.1016/0012-821X(78)90052-3.

Briggs, S. M., A. Yin, C. E. Manning, Z. L. Chen, X.-F. Wang, and M. Grove (2007), Late Paleozoic tectonic history of the Ertix Fault in the Chinese Altai and its implications for the development of the Central Asian Orogenic System, *Geol. Soc. Am. Bull.*, *119*(7–8), 944–960, doi:10.1130/b26044.1.

Briggs, S. M., A. Yin, C. E. Manning, Z. L. Chen, and X. F. Wang (2009), Tectonic development of the southern Chinese Altai Range as determined by structural geology, thermobarometry, $^{40}Ar/^{39}Ar$ thermochronology, and Th/Pb ion-microprobe monazite geochronology, *Geol. Soc. Am. Bull.*, *121*(9–10), 1381–1393, doi:10.1130/b26385.1.

Brown, S. J. A., R. M. Burt, J. W. Cole, S. J. P. Krippner, R. C. Price, and I. Cartwright (1998), Plutonic lithics in ignimbrites of Taupo Volcanic Zone, New Zealand; sources and conditions of crystallisation, *Chem. Geol.*, *148*(1–2), 21–41, doi:10.1016/s0009-2541(98)00026-6.

Buckman, S., and J. C. Aitchison (2004), Tectonic evolution of Palaeozoic terranes in West Junggar, Xinjiang, NW China, *Geol. Soc. London Spec. Publ.*, *226*(1), 101–129, doi:10.1144/gsl.sp.2004.226.01.06.

Buslov, M. M., I. Y. Saphonova, T. Watanabe, O. T. Obut, Y. Fujiwara, K. Iwata, N. N. Semakov, Y. Sugai, L. V. Smirnova, and A. Y. Kazansky (2001), Evolution of the Paleo-Asian Ocean (Altai-Sayan Region, Central Asia) and collision of possible Gondwana-derived terranes with the southern marginal part of the Siberian continent, *Geosci. J.*, *5*(3), 203–224, doi:10.1007/BF02910304.

Campos, T. F. C., F. H. R. Bezerra, N. K. Srivastava, M. M. Vieira, and C. Vita-Finzi (2010), Holocene tectonic uplift of the St Peter and St Paul Rocks (Equatorial Atlantic) consistent with emplacement by extrusion, *Mar. Geol.*, *271*(1–2), 177–186, doi:10.1016/j.margeo.2010.02.013.

Chen, B., and Y. Arakawa (2005), Elemental and Nd-Sr isotopic geochemistry of granitoids from the West Junggar foldbelt (NW China), with implications for Phanerozoic continental growth, *Geochim. Cosmochim. Acta*, *69*(5), 1307–1320, doi:10.1016/j.gca.2004.09.019.

Chen, B., and B. M. Jahn (2004), Genesis of post-collisional granitoids and basement nature of the Junggar Terrane, NW China: Nd-Sr isotope and trace element evidence, *J. Asian Earth Sci.*, *23*(5), 691–703, doi:10.1016/s1367-9120(03)00118-4.

Chen, J. F., B. F. Han, J. Q. Ji, L. Zhang, Z. Xu, G. Q. He, and T. Wang (2010), Zircon U-Pb ages and tectonic implications of Paleozoic plutons in northern West Junggar, North Xinjiang, China, *Lithos*, *115*(1–2), 137–152, doi:10.1016/j.lithos.2009.11.014.

Chen, S., and Z. J. Guo (2010), Time constraints, tectonic setting of Dalabute ophiolitic complex and its significance for Late Paleozoic tectonic evolution in West Junggar [in Chinese with English abstract], *Acta Petrol. Sin.*, *26*(8), 2336–2344.

Chen, S., Z. Guo, G. Pe-Piper, and B. Zhu (2013), Late Paleozoic peperites in West Junggar, China, and how they constrain regional tectonic and palaeoenvironmental setting, *Gondwana Res.*, *23*(2), 666–681, doi:10.1016/j.gr.2012.04.012.

Choulet, F., M. Faure, D. Cluzel, Y. Chen, W. Lin, and B. Wang (2012a), From oblique accretion to transpression in the evolution of the Altaid collage: New insights from West Junggar, northwestern China, *Gondwana Res.*, *21*(2–3), 530–547, doi:10.1016/j.gr.2011.07.015.

Choulet, F., M. Faure, D. Cluzel, Y. Chen, W. Lin, B. Wang, and B. M. Jahn (2012b), Architecture and evolution of accretionary orogens in the Altaids collage: The early Paleozoic West Junggar (NW China), *Am. J. Sci.*, *312*(10), 1098–1145, doi:10.2475/10.2012.02.

Choulet, F., D. Cluzel, M. Faure, W. Lin, B. Wang, Y. Chen, F. Y. Wu, and W. B. Ji (2012c), New constraints on the pre-Permian continental crust growth of Central Asia (West Junggar, China) by U–Pb and Hf isotopic data from detrital zircon, *Terra Nova*, *24*(3), 189–198, doi:10.1111/j.1365-3121.2011.01052.x.

Coleman, R. G. (1989), Continental growth of northwest China, *Tectonics*, *8*(3), 621–635, doi:10.1029/TC008i003p00621.

Collins, A. Q., K. E. Degtyarev, N. M. Levashova, M. L. Bazhenov, and R. Van der Voo (2003), Early Paleozoic paleomagnetism of east Kazakhstan: Implications for paleolatitudinal drift of tectonic elements within the Ural-Mongol belt, *Tectonophysics*, *377*(3–4), 229–247, doi:10.1016/j.tecto.2003.09.003.

Compston, W., I. S. Williams, and C. Meyer (1984), U-Pb geochronology of zircons from lunar breccia 73217 using a sensitive high mass-resolution ion microprobe, *J. Geophys. Res.*, *89*(S02), B525–B534, doi:10.1029/JB089iS02p0B525.

Dewey, J. F. (1977), Suture zone complexities: A review, *Tectonophysics*, *40*(1–2), 53–67, doi:10.1016/0040-1951(77)90029-4.

Dewey, J. F. (2005), Orogeny can be very short, *Proc. Natl. Acad. Sci. U.S.A.*, *102*(43), 15,286–15,293, doi:10.1073/pnas.0505516102.

Feng, Y., R. G. Coleman, G. Tilton, and X. Xiao (1989), Tectonic evolution of the West Junggar Region, Xinjiang, China, *Tectonics*, *8*(4), 729–752, doi:10.1029/TC008i004p00729.

Festa, A., G. A. Pini, Y. Dilek, and G. Codegone (2010), Mélanges and mélange-forming processes: A historical overview and new concepts, *Int. Geol. Rev.*, *52*(10–12), 1040–1105, doi:10.1080/00206810903557704.

Gansser, A. (1974), The ophiolitic mélange, a world-wide problem on Tethyan examples, *Ecologgae Geol. Helvetiae*, *67*(3), 479–507.

Geng, H. Y., M. Sun, C. Yuan, W. Xiao, W. Xian, G. Zhao, L. Zhang, K. Wong, and F. Wu (2009), Geochemical, Sr-Nd and zircon U-Pb-Hf isotopic studies of Late Carboniferous magmatism in the West Junggar, Xinjiang: Implications for ridge subduction?, *Chem. Geol.*, *266*(3–4), 364–389, doi:10.1016/j.chemgeo.2009.07.001.

Geng, H. Y., M. Sun, C. Yuan, G. C. Zhao, and W. J. Xiao (2011), Geochemical and geochronological study of early Carboniferous volcanic rocks from the West Junggar: Petrogenesis and tectonic implications, *J. Asian Earth Sci.*, *42*(5), 854–866, doi:10.1016/j.jseaes.2011.01.006.

Gu, P. Y., Y. J. Li, B. Zhang, L. L. Tong, and J. N. Wang (2009), LA-ICP-MS zircon U–Pb dating of gabbro in the Darbut ophiolite, western Junggar, China [in Chinese with English abstract], *Acta Petrol. Sin.*, *25*(6), 1364–1372.

Guo, L. S., R. Zhang, Y. L. Liu, F. J. Xu, and L. Su (2009), Zircon U-Pb age of Tonghualing intermediate-acid intrusive rocks, Eastern Junggar, Xinjiang [in Chinese with English abstract], *Acta Sci. Nat. Univ. Pekingensis*, *45*(5), 819–824.

Guo, L. S., Y. L. Liu, Z. H. Wang, D. Song, F. J. Xu, and L. Su (2010), The Zircon U-Pb LA-ICP-MS Geochronology of volcanic rocks in Baogutu areas, Western Junggar [in Chinese with English abstract], *Acta Petrol. Sin.*, *26*(2), 471–478.

Han, B. F., J. Q. Ji, B. Song, L. H. Chen, and L. Zhang (2006), Late Paleozoic vertical of continental crust around the Junggar Basin, Xinjiang, China (Part I): Timing of post-collisional plutonism [in Chinese with English abstract], *Acta Petrol. Sin.*, *22*(5), 1077–1086.

Han, B. F., Z. J. Guo, Z. C. Zhang, L. Zhang, J. F. Chen, and B. Song (2010), Age, geochemistry, and tectonic implications of a late Paleozoic stitching pluton in the North Tian Shan suture zone, western China, *Geol. Soc. Am. Bull.*, *122*(3–4), 627–640, doi:10.1130/b26491.1.

Jahn, B.-M. (2004), The Central Asian Orogenic Belt and growth of the continental crust in the Phanerozoic, *Geol. Soc. London Spec. Publ.*, *226*(1), 73–100, doi:10.1144/GSL.SP.2004.226.01.05.

Jin, C. W., and X. Q. Zhang (1993), A geochronology and geneses of the weatern Junggar granitoids, Xinjiang, China [in Chinese with English abstract], *Sci. Geol. Sin.*, *28*(1), 28–36.

Kapp, P., M. A. Murphy, A. Yin, T. M. Harrison, L. Ding, and J. Guo (2003), Mesozoic and Cenozoic tectonic evolution of the Shiquanhe area of western Tibet, *Tectonics*, *22*(4), 1029, doi:10.1029/2001TC001332.

Kimura, G., S. Maruyama, Y. Isozaki, and M. Terabayashi (1996), Well-preserved underplating structure of the jadeitized Franciscan complex, Pacheco Pass, California, *Geology*, *24*(1), 75–78, doi:10.1130/0091-7613(1996)024<0075:wpusot>2.3.co;2.

Kusky, T. M., and D. C. Bradley (1999), Kinematic analysis of mélange fabrics: Examples and applications from the McHugh Complex, Kenai Peninsula, Alaska, *J. Struct. Geol.*, *21*(12), 1773–1796, doi:10.1016/S0191-8141(99)00105-4.

Levashova, N. M., K. E. Degtyarev, M. L. Bazhenov, A. Q. Collins, and R. Van der Voo (2003), Middle Paleozoic paleomagnetism of east Kazakhstan: Post-Middle Devonian rotations in a large-scale orocline in the central Ural-Mongol belt, *Tectonophysics*, *377*(3–4), 249–268, doi:10.1016/j.tecto.2003.09.013.

Levashova, N. M., K. E. Degtyarev, and M. L. Bazhenov (2012), Oroclinal bending of the Middle and Late Paleozoic volcanic belts in Kazakhstan: Paleomagnetic evidence and geological implications, *Geotectonics*, *46*(4), 285–302, doi:10.1134/S0016852112030041.

Li, J. Y. (1995), Main characteristics and emplacement processes of the east junggar ophiolites, Xinjiang, China [in Chinese with English abstract], *Acta Petrol. Sin.*, *11*(S1), 74–84.

Li, J. Y., X. C. Xiao, and W. Chen (2000), Late Ordovician continental basement of the eastern Junggar Basin in Xinjiang, NW China: Evidence from the Laojunmiao metamorphic complex on the northeast basin margin [in Chinese with English abstract], *Reg. Geol. China*, *19*(3), 297–302.

Li, Y. P., J. Y. Li, G. H. Sun, Z. X. Zhu, and Z. Q. Yang (2007), Basement of Junggar basin: Evidence from detrital zircons in sandstone of previous Devonian Kalamaili formation [in Chinese with English abstract], *Acta Petrol. Sin.*, *23*(7), 1577–1590.

Li, Y. P., J. Y. Li, G. H. Sun, Z. X. Zhu, and B. Song (2009), Determination of the Early Devonian granite in East Junggar, Xinjiang, China and its geological implications [in Chinese with English abstract], *Geol. Bull. China*, *28*(12), 1885–1993.

Liu, Y. L., L. S. Guo, Y. D. Liu, H. X. Song, B. Song, R. Zhang, F. J. Xu, and Y. X. Zhang (2009), Geochronology of Baogutu porphyry copper deposit in Western Junggar area, Xinjiang of China, *Sci. China, Ser. D: Earth Sci.*, *52*(10), 1543–1549, doi:10.1007/s11430-009-0127-7.

McNulty, B. A., D. L. Farber, G. S. Wallace, R. Lopez, and O. Palacios (1998), Role of plate kinematics and plate-slip-vector partitioning in continental magmatic arcs: Evidence from the Cordillera Blanca, Peru, *Geology*, *26*(9), 827–830, doi:10.1130/0091-7613(1998)026<0827:ropkap>2.3.co;2.

Meng, J. F., Z. J. Guo, and S. H. Fang (2009), A new insight into the thrust structures at the northwestern margin of Junggar Basin [in Chinese with English abstract], *Earth Sci. Front.*, *16*(3), 171–180.

Orange, D. L. (1990), Criteria helpful in recognizing shear-zone and diapiric mélanges: Examples from the Hoh accretionary complex, Olympic Peninsula, Washington, *Geol. Soc. Am. Bull.*, *102*(7), 935–951, doi:10.1130/0016-7606(1990)102<0935:chirsz>2.3.co;2.

Polat, A., and R. Kerrich (1999), Formation of an Archean tectonic méange in the Schreiber-Hemlo greenstone belt, Superior Province, Canada: Implications for Archean subduction-accretion process, *Tectonics*, *18*(5), 733–755, doi:10.1029/1999TC900032.

Ramsay, J. G. (1980), The crack-seal mechanism of rock deformation, *Nature*, *284*(5752), 135–139, doi:10.1038/284135a0.

Ren, R., et al. (2014), When did the subduction first initiate in the southern Paleo-Asian Ocean: New constraints from a Cambrian intra-oceanic arc system in West Junggar, NW China, *Earth Planet. Sci. Lett.*, *388*, 222–236, doi:10.1016/j.epsl.2013.11.055.

Saleeby, J. B. (1984), Tectonic significance of serpentinite mobility and ophiolite melange, in *Melanges: Their Nature, Origin, and Significance*, *Geol. Soc. Am., Spec. Pap.*, vol. 198, edited by L. A. Raymond, pp. 153–168, GSA, Boulder, Colo.

Şengör, A. M. C. (1992), The Palaeo-Tethyan suture: A line of demarcation between two fundamentally different architectural styles in the structure of Asia, *Island Arc*, *1*(1), 78–91, doi:10.1111/j.1440-1738.1992.tb00060.x.

Şengör, A. M. C., and B. A. Natal'in (1996), Turkic-type orogeny and its role in the making of the continental crust, *Annu. Rev. Earth Planet. Sci.*, *24*(1), 263–337, doi:10.1146/annurev.earth.24.1.263.

Şengör, A. M. C., B. A. Natal'in, and V. S. Burtman (1993), Evolution of the Altaid tectonic collage and Paleozoic crustal growth in Eurasia, *Nature*, *364*(6435), 299–307, doi:10.1038/364299a0.

Shabanian, E., V. Acocella, A. Gioncada, H. Ghasemi, and O. Bellier (2012), Structural control on volcanism in intraplate post collisional settings: Late Cenozoic to Quaternary examples of Iran and Eastern Turkey, *Tectonics*, *31*, Tc3013, doi:10.1029/2011TC003042.

Shu, L. S., and Y. J. Wang (2003), Late Devonian-Early Carboniferous radiolarian fossils from siliceous rocks of the Kalamaili ophiolite, Xinjiang [in Chinese with English abstract], *Geol. Rev.*, *49*(4), 408–412.

Simpson, C., and S. M. Schmid (1983), An evaluation of criteria to deduce the sense of movement in sheared rocks, *Geol. Soc. Am. Bull.*, *94*(11), 1281–1288, doi:10.1130/0016-7606(1983)94<1281:AEOCTD>2.0.CO;2.

Smith, A. B., and M. Colchen (1988), Late Palaeozoic biogeography of East Asia and palaeontological constraints on plate tectonic reconstructions [and discussion], *Philos. Trans. R. Soc., A*, *326*(1589), 189–227, doi:10.1098/rsta.1988.0085.

Sylvester, A. G. (1988), Strike-slip faults, *Geol. Soc. Am. Bull.*, *100*(11), 1666–1703, doi:10.1130/0016-7606(1988)100<1666:ssf>2.3.co;2.

Tang, G. J., Q. Wang, D. A. Wyman, Z.-X. Li, Z.-H. Zhao, X.-H. Jia, and Z.-Q. Jiang (2010), Ridge subduction and crustal growth in the Central Asian Orogenic Belt: Evidence from Late Carboniferous adakites and high-Mg diorites in the western Junggar region, northern Xinjiang (west China), *Chem. Geol.*, *277*(3–4), 281–300, doi:10.1016/j.chemgeo.2010.08.012.

Tang, H. F., Y. P. Su, C. Q. Liu, G. S. Hou, and Y. B. Wang (2007), Zircon U-Pb age of the plagiogranite in Kalamaili belt, northern Xinjiang and its tectonic implications [in Chinese with English abstract], *Geotecton. Metallog.*, *31*(1), 110–117.

Tong, L. L., Y. J. Li, B. Zhang, J. Liu, Z. J. Pang, and J. N. Wang (2009), Zircon LA-ICP-MS U-Pb dating and geologic age of the Baogutu formation andesite in the south of Dalabute faulted zone, Western Junggar [in Chinese with English abstract], *Xinjiang Geol.*, *27*(3), 226–230.

van der Pluijm, B. A., and S. Marshak (1997), *Earth Structure: An Introduction to Structural Geology and Tectonics*, 1st ed., W.W. Norton, New York.

Windley, B. F., D. Alexeiev, W. Xiao, A. Kroner, and G. Badarch (2007), Tectonic models for accretion of the Central Asian Orogenic Belt, *J. Geol. Soc.*, *164*(1), 31–47, doi:10.1144/0016-76492006-022.

Xiao, W. J., B. F. Windley, J. Hao, and M. G. Zhai (2003), Accretion leading to collision and the Permian Solonker suture, Inner Mongolia, China: Termination of the central Asian orogenic belt, *Tectonics*, *22*(6), 1069, doi:10.1029/2002TC001484.

Xiao, W. J., B. F. Windley, G. Badarch, S. Sun, J. L. Li, K. Z. Qin, and Z. H. Wang (2004a), Palaeozoic accretionary and convergent tectonics of the southern Altaids: Implications for the growth of Central Asia, *J. Geol. Soc.*, *161*(3), 339–342, doi:10.1144/0016-764903-165.

Xiao, W. J., L. C. Zhang, K. Z. Qin, S. Sun, and J. L. Li (2004b), Paleozoic accretionary and collisional tectonics of the eastern Tianshan (China): Implications for the continental growth of central Asia, *Am. J. Sci.*, *304*(4), 370–395, doi:10.2475/ajs.304.4.370.

Xiao, W. J., C. M. Han, C. Yuan, M. Sun, S. F. Lin, H. L. Chen, Z. L. Li, J. L. Li, and S. Sun (2008), Middle Cambrian to Permian subduction-related accretionary orogenesis of Northern Xinjiang, NW China: Implications for the tectonic evolution of central Asia, *J. Asian Earth Sci.*, *32*(2–3), 102–117, doi:10.1016/j.jseaes.2007.10.008.

Xiao, W. J., B. C. Huang, C. M. Han, S. Sun, and J. L. Li (2010), A review of the western part of the Altaids: A key to understanding the architecture of accretionary orogens, *Gondwana Res.*, *18*(2–3), 253–273, doi:10.1016/j.gr.2010.01.007.

Xiao, W. J., C. M. Han, W. Liu, B. Wan, J. E. Zhang, S. J. Ao, Z. Y. Zhang, D. F. Song, Z. H. Tian, and J. Luo (2014), How many sutures in the southern Central Asian Orogenic Belt: Insights from East Xinjiang–West Gansu (NW China)?, *Geosci. Front.*, *5*(4), 525–536, doi:10.1016/j.gsf.2014.04.002.

Xu, Q. Q., J. Q. Ji, J. F. Gong, L. Zhao, J. Y. Tu, D. X. Sun, T. Tao, Z. H. Zhu, G. Q. He, and J. J. Hou (2009), Structural style and deformation sequence of western Junggar, Xinjiang, since Late Paleozoic [in Chinese with English abstract], *Acta Petrol. Sin.*, *25*(3), 636–644.

Xu, X. Y., Z. P. Ma, L. Q. Xia, Y. B. Wang, X. M. Li, Z. C. Xia, and L. S. Wang (2005), SHRIMP dating of plagiogranite from Bayingou ophiolite in the northern Tianshan Mountains [in Chinese with English abstract], *Geol. Rev.*, *51*(5), 523–527.

Xu X. Y., et al. (2006a), LA-ICPMS zircon U-Pb dating of gabbro from the Bayingou ophiolite in the northern Tianshan Mountains [in Chinese], *Acta Geol. Sin.*, *80*, 1168–1176.

Xu, X., G. Q. He, H. Q. Li, T. F. Ding, X. Y. Liu, and S. W. Mei (2006b), Basic characteristics of the Karamay ophiolitic mélange, Xinjiang, and its zircon SHRIMP dating [in Chinese with English abstract], *Geol. China*, *33*(3), 470–475.

Xu, Z., B. F. Han, R. Ren, Y. Z. Zhou, L. Zhang, J. F. Chen, L. Su, X. H. Li, and D. Y. Liu (2012), Ultramafic-mafic mélange, island arc and post-collisional intrusions in the Mayile Mountain, West Junggar, China: Implications for Paleozoic intra-oceanic subduction-accretion process, *Lithos*, *132–133*, 141–161, doi:10.1016/j.lithos.2011.11.016.

Yakubchuk, A. (2004), Architecture and mineral deposit settings of the Altaid orogenic collage: A revised model, *J. Asian Earth Sci.*, *23*(5), 761–779, doi:10.1016/j.seaes.2004.01.006.

Yang, G. X., Y. J. Li, P. Y. Gu, B. K. Yang, L. L. Tong, and H. W. Zhang (2012a), Geochronological and geochemical study of the Darbut Ophiolitic Complex in the West Junggar (NW China): Implications for petrogenesis and tectonic evolution, *Gondwana Res.*, *21*(4), 1037–1049, doi:10.1016/j.gr.2011.07.029.

Yang, G. X., Y. J. Li, M. Santosh, B. K. Yang, J. Yan, B. Zhang, and L. L. Tong (2012b), Geochronology and geochemistry of basaltic rocks from the Sartuohai ophiolitic mélange, NW China: Implications for a Devonian mantle plume within the Junggar Ocean, *J. Asian Earth Sci.*, *59*(0), 141–155, doi:10.1016/j.jseaes.2012.07.020.

Yi, Z. Y., B. C. Huang, W. J. Xiao, L. K. Yang, and Q. Q. Qiao (2013), Paleomagnetic study of Late Paleozoic rocks in the Tacheng Basin of West Junggar (NW China): Implications for the tectonic evolution of the western Altaids, *Gondwana Res.*, doi:10.1016/j.gr.2013.11.006.

Yin, A., and T. M. Harrison (2000), Geologic evolution of the Himalayan-Tibetan Orogen, *Annu. Rev. Earth Planet. Sci.*, *28*(1), 211–280, doi:10.1146/annurev.earth.28.1.211.

Yin, A., C. E. Manning, O. Lovera, C. A. Menold, X. H. Chen, and G. E. Gehrels (2007), Early paleozoic tectonic and thermomechanical evolution of ultrahigh-pressure (UHP) metamorphic rocks in the northern Tibetan Plateau, northwest China, *Int. Geol. Rev.*, *49*(8), 681–716, doi:10.2747/0020-6814.49.8.681.

Yin, J. Y., C. Yuan, M. Sun, X. P. Long, G. C. Zhao, K. P. Wong, H. Y. Geng, and K. D. Cai (2010), Late Carboniferous high-Mg dioritic dikes in Western Junggar, NW China: Geochemical features, petrogenesis and tectonic implications, *Gondwana Res.*, *17*(1), 145–152, doi:10.1016/j.gr.2009.05.011.

Zhang, C., and X. Huang (1992), Age and tectonic settings of ophiolites in west Junggar, Xinjiang [in Chinese with English abstract], *Geol. Rev.*, *38*(6), 509–524.

Zhang, J. E., W. J. Xiao, C. M. Han, S. J. Ao, C. Yuan, M. Sun, H. Y. Geng, G. C. Zhao, Q. Q. Guo, and C. Ma (2011a), Kinematics and age constraints of deformation in a Late Carboniferous accretionary complex in Western Junggar, NW China, *Gondwana Res.*, *19*(4), 958–974, doi:10.1016/j.gr.2010.10.003.

Zhang, J. E., W. J. Xiao, C. M. Han, Q. G. Mao, S. J. Ao, Q. Q. Guo, and C. Ma (2011b), A Devonian to Carboniferous intra-oceanic subduction system in Western Junggar, NW China, *Lithos*, *125*(1–2), 592–606, doi:10.1016/j.lithos.2011.03.013.

Zhang, L. F. (1997), $^{40}Ar/^{39}Ar$ age of blueschists in Tangbale, Western Junggar, Xinjiang, and its significance [in Chinese with English abstract], *Chin. Sci. Bull.*, *42*, 2178–2181.

Zhang, Y. Y., and Z. J. Guo (2010), New constraints on formation ages of ophiolites in northern Junggar and comparative study on their connection [in Chinese with English abstract], *Acta Petrol. Sin.*, *26*(2), 421–430.

Zhang, Y. Y., G. Pe-Piper, D. J. W. Piper, and Z. J. Guo (2013), Early Carboniferous collision of the Kalamaili orogenic belt, North Xinjiang and its implications: Evidence from molasse deposits, *Geol. Soc. Am. Bull.*, *125*(5–6), 932–944, doi:10.1130/B30779.1.

Zheng, J. P., M. Sun, G. C. Zhao, P. T. Robinson, and F. Z. Wang (2007), Elemental and Sr-Nd-Pb isotopic geochemistry of Late Paleozoic volcanic rocks beneath the Junggar basin, NW China: Implications for the formation and evolution of the basin basement, *J. Asian Earth Sci.*, *29*(5–6), 778–794, doi:10.1016/j.jseaes.2006.05.004.

Zhu, Y. F., and X. Xu (2006), The discovery of Early Ordovician ophiolite mélange in Taerbahatai Mountains, Xinjiang, NW China [in Chinese with English abstract], *Acta Petrol. Sin.*, *22*(12), 2833–2842.

Zhu, Y. F., X. Xu, S. N. Wei, B. Song, and X. Guo (2007), Geochemistry and tectonic significance of OIB-type pillow basalts in western Mts. of Karamay city (western Junggar), NW China [in Chinese with English abstract], *Acta Petrol. Sin.*, *24*(12), 2767–2777.